

**UCSF**

**UC San Francisco Electronic Theses and Dissertations**

**Title**

Brain to blood acid transport

**Permalink**

<https://escholarship.org/uc/item/1k4844st>

**Author**

Gonzalez, Mario Alberto

**Publication Date**

1975

Peer reviewed|Thesis/dissertation

BRAIN TO BLOOD ACID TRANSPORT:  
KINETICS AND INHIBITION

by

Mario Alberto Gonzalez  
B.S., University of Texas 1964  
M.S., University of Texas 1967

DISSERTATION

Submitted in partial satisfaction of the requirements for the degree of

DOCTOR OF PHILOSOPHY

in

PHARMACEUTICAL CHEMISTRY

in the

GRADUATE DIVISION

(San Francisco)



© 1975

MARIO ALBERTO GONZÁLEZ

ALL RIGHTS RESERVED

## ABSTRACT

Different organic acids have been shown to block the transfer of 5-hydroxyindoleacetic acid (5HIAA) from the brain. This blockade was proposed to involve inhibition of a carrier-mediated transport system for 5HIAA elimination.

A model based on transport kinetics and competitive inhibition was developed to simulate the levels of brain 5HIAA after an inhibitor. To test this model rats were sacrificed at different times following a single dose of probenecid. The brains were assayed for 5HIAA by fluorescence and for probenecid by gas-liquid chromatography. Plasma concentrations of probenecid were also determined by gas-liquid chromatography. An analog computer was used to fit the model to the 5HIAA brain level-time curves by varying the constant of inhibition,  $K_I$ . The  $K_I$  obtained from the curve of best fit was time independent and only one dose was required as opposed to that of the usual dose-response determinations.  $K_I$  was determined in this fashion for doses of 100 and 300 mg/kg. The constant of inhibition was also calculated by an alternate procedure. Determination of the inhibitor concentration in the brain and plasma allowed a comparison of the calculated percent inhibition with the inhibitor concentration yielding the concentration of probenecid which produced 50 percent inhibition, that is,  $K_I$ .

It was further proposed that the acid elimination system prevents the equilibration of slowly diffusible

exogenous acids between brain and plasma. In effect, the transport system contributes to the "Blood-Brain Barrier."

To test this concept, a model was developed to detect nonlinear disposition of a drug in a tissue. The model was experimentally tested as it relates to salicylic acid disposition in the brain. Experimental data were obtained in rats for intraperitoneal doses of 25 and 400 mg/kg. The parameters measured for each dose were the ratio of the area under the brain concentration-time curve to the area under the plasma concentration-time curve and the ratio of the maximum brain concentration of salicylic acid to the plasma concentration at the time the brain levels were maximal. The ratios were seen to increase with dose. Ratios calculated using plasma concentrations corrected for plasma protein binding were also dose-dependent. Calculations performed on literature data for salicylic acid disposition in mouse brain corroborate the results of this study. Facilitated transport of salicylic acid out of mouse and rat brain was proposed to explain the nonlinear disposition.

Thus, the existence of a saturable, carrier-mediated acid transport system for the elimination of both endogenous and exogenous acids from the brain is supported by the data presented.

## ACKNOWLEDGMENTS

A student who has had the pleasure of attending this University faces a difficult task when it comes to writing his acknowledgments. Surely the School of Pharmacy is endowed with a fantastic faculty headed by Dean Goyan. Dr. Riegelman has been a helpful critic and a kind advisor. Dr. Sutherland had the patience to suggest approaches to my learning and research even before I knew what my research would be. Dr. Tozer was so much more than a supervising professor that I will never be able to thank him enough. Gracias a todos.

The author acknowledges receipt of a U. S. Public Health Service Traineeship (5T01 GM006728-07).

To the Grahams and the Gonzalezes

## TABLE OF CONTENTS

CHAPTER		PAGE
I	INTRODUCTION . . . . .	1
II	TRANSPORT OF 5HIAA FROM THE BRAIN . .	8
	Section 1: Introduction . . . . .	8
	Section 2: Theoretical . . . . .	10
	Section 3: Experimental . . . . .	16
	Section 4: Results and Discussion .	28
III	TRANSPORT OF SALICYLIC ACID FROM THE	
	BRAIN . . . . .	56
	Section 1: Introduction . . . . .	56
	Section 2: Theoretical . . . . .	57
	Section 3: Experimental . . . . .	67
	Section 4: Results and Discussion .	70
IV	SUMMARY AND CONCLUSIONS . . . . .	83
	APPENDIX A: MODEL AND ANALOG COMPUTER	
	DIAGRAM USED IN THE DETERMINATION OF	
	$K_I$ . . . . .	95
	APPENDIX B: CORRECTION FOR RESIDUAL	
	BLOOD IN BRAIN . . . . .	98
	BIBLIOGRAPHY . . . . .	104



## LIST OF TABLES

TABLE		PAGE
I	Rat Brain 5HIAA Concentrations after Intraperitoneal Doses of Probenecid .	29
II	Rat Plasma and Brain Probenecid Levels after a 100 mg/kg Intraperitoneal Dose of Probenecid . . . . .	30
III	Rat Plasma and Brain Probenecid Levels after a 300 mg/kg Intraperitoneal Dose of Probenecid . . . . .	31
IV	Rat Plasma Probenecid Concentrations after 100 and 200 mg/kg Intraperitoneal Doses of Probenecid . . . . .	32
V	Probenecid Half Lives after Different Doses . . . . .	33
VI	Constants of Inhibition ( $K_I$ 's) Calculated from Computer Fits of 5HIAA Data . . . . .	36
VII	Calculated Percent Inhibition Values after Intraperitoneal Doses of Probenecid . . . . .	40
VIII	Percent Inhibition Values with Corresponding Probenecid Plasma Concentrations . . . . .	42
IX	Salicylic Acid Disposition in the Rat Brain and Plasma . . . . .	71
X	Experimentally Determined Distribution Ratios . . . . .	74
XI	Distribution Ratios for Salicylic Acid in Mice . . . . .	75
XII	Blood and Plasma Concentrations upon Adding Salicylic Acid to Rat Blood .	100

## LIST OF FIGURES

FIGURE		PAGE
2-1	Rat brain 5HIAA concentrations after a 100 mg/kg intraperitoneal dose of probenecid . . . . .	44
2-2	Standard curve for 5HIAA . . . . .	45
2-3	Standard curve for probenecid extracted from rat plasma. . . . .	46
2-4	Gas-liquid chromatography recording for extractions of probenecid from rat plasma . . . . .	47
2-5	Gas-liquid chromatography recording for extractions of probenecid from rat brain . . . . .	48
2-6	Semi-logarithmic plots of rat plasma and brain probenecid levels after a 100 mg/kg intraperitoneal dose of probenecid . . . . .	49
2-7	Semi-logarithmic plots of rat plasma and brain probenecid levels after a 300 mg/kg intraperitoneal dose of probenecid . . . . .	50
2-8	Semi-logarithmic plots of rat plasma probenecid concentrations after 100 and 200 mg/kg intraperitoneal doses of probenecid . . . . .	51
2-9	Rat brain 5HIAA levels, expressed as percent of control, following a 100 mg/kg intraperitoneal dose of probenecid . . . . .	52
2-10	Rat brain 5HIAA levels, expressed as percent of control, following a 100 mg/kg intraperitoneal dose of probenecid . . . . .	53
2-11	Rat brain 5HIAA levels, expressed as percent of control, following a 300 mg/kg intraperitoneal dose of probenecid . . . . .	54

FIGURE		PAGE
2-12	Calculated percent inhibition values versus the logarithm of the corresponding probenecid plasma concentrations . . . . .	55
3-1	Schematic diagram of the processes of disposition of a drug in the brain or any tissue . . . . .	78
3-2	Standard curve for salicylic acid extracted from rat plasma . . . . .	79
3-3	Standard curve for salicylic acid extracted from rat brain . . . . .	80
3-4	Unbound fraction of total plasma concentration, $\alpha_1$ , as a function of the total plasma concentration, $C_p$ . . . .	81
3-5	Semi-logarithmic plots of salicylic acid concentrations in rat brain and plasma versus time after intraperitoneal administration of 25 and 400 mg/kg. . . .	82
4-1	Analog computer curves representing 5HIAA brain levels as a function of time . . . . .	94
A-1	Analog computer diagram used to represent the change in 5HIAA brain levels after a dose of probenecid . . . . .	97
B-1	Ratio of salicylic acid blood concentration ( $C_B$ ) to plasma concentration ( $C_p$ ) as a function of the fraction of drug unbound in the plasma ( $\alpha_1$ ) . . . . .	103

## CHAPTER I

### INTRODUCTION

The brain has long been noted to be more resistant than other tissues to the penetration of certain compounds. This phenomenon, frequently referred to as the blood-brain barrier, was first detected when acid dyes were seen not to pass from the blood to the brain despite high blood concentrations of the dyes (1, 2). It could be argued that acid dyes such as trypan blue would be poor indicators of a blood-brain barrier, since these compounds are very highly bound to proteins in the blood and thus their diffusion into tissues would be inhibited. Yet trypan blue will readily stain most tissues of an animal while the central nervous system remains virtually unaffected (3).

The first quantitative studies of the blood-brain barrier were carried out by Wallace and Brodie (4). Brodie and his co-workers carried out extensive studies which showed that many diverse compounds entered the brain at a slower rate than that observed in other tissues (5). These studies also demonstrated that highly lipophilic compounds were capable of rapid penetration of the central nervous system (6). The logical conclusion from these results was to attribute lipid characteristics to the blood-brain barrier much like those of most membranes. The drug penetration of the brain would thus depend upon the lipophilic properties of the compound and its

degree of ionic dissociation. These conclusions although valid did not explain the marked difference in drug entry between the brain and other tissues with similar blood perfusions.

An early postulate to explain the barrier effect was the lack of a sufficient extracellular space in the brain to allow the diffusion of plasma borne compounds into the brain. Electron microscopists estimated an extracellular space in the brain of only 5% or less (7). This view, however, is not currently acceptable, since subsequent physiological experiments have shown this space to be as high as 15-20% (8). The obstacle to entry into the brain is most likely the result of differences in the capillaries of the brain. Whereas in other tissues the capillaries are surrounded by extracellular fluid, brain capillaries are covered by the end-feet of the astrocytes or glial cells (9). Thus the astrocytic protoplasm constitutes an extra barrier which a molecule in the blood must cross before reaching the brain. Another notable anatomical difference which makes the brain capillaries unlike those of other tissues is the existence of continuous tight intercellular junctions in the capillary endothelial cells (10). The absence of any intercellular space in the endothelium requires a drug in the blood to diffuse through the endothelial cell itself, while in other tissues a compound might be capable of diffusing through spaces 50-100 Å wide.

Conceivably, the observed anatomical differences in the capillaries of the brain explain why certain compounds enter the central nervous system at a slower rate than that observed in other tissues. It would not explain, however, why the

unbound concentrations of some compounds do not achieve equilibrium between plasma and brain even when the plasma concentration is maintained constant by infusion. Mayer, et al. (5) showed that salicylic acid in the brains of rabbits did not achieve equilibrium with the unbound drug in the plasma although the plasma concentration was maintained at steady state for three hours. Kleeman, et al. (11) demonstrated a similar occurrence with urea; after three hours of infusion the drug in the brain reached a plateau which was one-half of the plasma concentration. Anatomical differences alone could not explain the results of these experiments; however, the existence of a transport mechanism in the direction of brain to blood might explain the unequal distribution of some drugs between blood and brain. Evidence for such a transport system which would function as a component of the blood-brain barrier has been reviewed (11, 12). Steinwall (13) proposed the existence of a transport system for organic acids in the brain. He showed that acid dyes which normally did not enter the central nervous system could be made to cross the barrier by the administration of various metabolic inhibitors. Hypothermia and high concentrations of other organic acids also induced extravasation of the acid dyes into the brain. The conclusions from this work were that acid dyes apparently do not penetrate the brain from the blood because of a transport system which operates in the opposite direction. Drawing an analogy with the kidney, he proposed that such a transport system would not only protect the central nervous system from

toxic acids in the blood, but would also serve in an excretory capacity to rid the brain of unwanted or toxic acidic metabolites formed within the brain.

In view of Steinwall's theory, the inability of salicylic acid in the brain to achieve equal concentration with the unbound drug in the plasma (5) could be interpreted to be proof of the existence of an acid transport system in the brain. A unidirectional mechanism which was capable of transporting acids from the brain to the blood would account for the salicylate concentration in the brain remaining lower than the unbound concentration in the plasma. Similar evidence can be found in an early study with penicillin-G in which equivalent concentrations in the cerebrospinal fluid (CSF) and plasma of man were never achieved even under conditions of continuous administration (14). Further evidence for the existence of an acid transport system is the report that increasing doses of ampicillin result in disproportionate increases in the CSF concentration of the drug in dogs (15). This is consistent with the concept of a saturable transport system; as the dose increases the result is a lowering of the rate of elimination relative to the amount in the tissue. Ampicillin levels in the CSF would then increase more than the corresponding increase in the plasma concentrations. Conclusive evidence has also been presented by Fishman (16) to substantiate that penicillin-G is transported out of the CSF of dogs. The transport which appeared unidirectional exhibited saturability, and it was inhibited by

probenecid, a well known acid transport inhibitor. The acidic compounds Diodrast and phenolsulfonphthalein have also been shown to be actively transported out of the CSF of goats (17). The ventricles and cisterna magna were perfused with a solution of either Diodrast or phenolsulfonphthalein, and the passage of the test compound from CSF to blood was found to be unidirectional, capable of saturation, and sensitive to inhibition by para-aminohippurate.

The foregoing discussion has been concerned with the transport of exogenous compounds from the brain, that is, compounds which normally are not found in the central nervous system. There is indication, however, that acids produced in the brain (endogenous acids) are also eliminated from the brain via a transport system. Probenecid and other organic acids have been shown to block the efflux of 5-hydroxyindoleacetic acid (5HIAA), one of the end products of serotonin metabolism in the brain (18-20). The transport of 5 HIAA out of the brain appears to be unidirectional, since intravenous doses of the compound produced no changes in the CSF levels of 5HIAA in dogs (21). Despite the fact that 5HIAA does not readily enter the brain, it appears to leave the brain with little difficulty, since the fractional turnover rate in brain is 85% per hour (20). This also suggests a transport system, since diffusion is too slow a process to account for such a rapid fractional turnover rate. The administration of a monamine oxidase inhibitor which blocks 5HIAA synthesis produces a drop in the 5HIAA levels in the brain, but an



efflux inhibitor administered concomitantly with the monoamine oxidase inhibitor prevents the drop in the 5HIAA levels (19). Support is thus given to the transport theory, since 5HIAA does not appear to leave the brain passively in a significant amount. A transport for 5HIAA has also been demonstrated in cat CSF (22) and in the dog (23,24).

There is evidence that the acid transport system is not very specific. Different acidic compounds such as probenecid, phenylacetic acid, and benzoic acid inhibit the elimination of 5HIAA (20, 25). It is probable that the lack of specificity extends to the compounds being transported and not just the inhibitors. Homovanillic acid, an acidic end product of dopamine metabolism in the brain, also appears to be transported (23). The transport inhibitors which block 5HIAA transport also block the efflux of homovanillic acid (23, 25). Referring again to Steinwall's proposal (13), it seems reasonable that a transport system should exist for removing unwanted and potentially toxic compounds from the brain. It is very likely that such a system should be non-specific so that it may function in removing both endogenous and exogenous acidic compounds. This transport system would be of physiologic importance in removing potentially toxic polar acid metabolites formed within the brain and in preventing the accumulation of exogenous polar organic acids in the central nervous system.

With few exceptions most of the studies involving brain transport have utilized ventricular-cisternal perfusions or the incubation of brain slices or of isolated choroid plexuses. The drawbacks of an in vitro study are many, the most important of which is the possibility that the barrier effect may be lost in removing the brain from the animal. With brain perfusion studies, an intact animal is used, but it might not be representative of a normal animal after the necessary surgery, restraint, and loss of CSF. Furthermore, transport from the CSF into the blood may not be representative of the total brain, since transport could occur directly from the brain parenchyma into the blood without CSF involvement. The use of perfusion techniques to introduce foreign compounds into the brain is also questionable, since the normal mode of entry into the brain is ignored.

The objective of the present investigation is to study in vivo the brain's acid transport system in intact animals and to demonstrate that the inability of many acids to pass from blood to brain is due, at least partly, to an acid transport system from the brain to the blood. To meet this objective, the transport of endogenous and exogenous organic acids was studied. The indole metabolite, 5-hydroxyindoleacetic acid, was used to study the transport of an endogenous acid; salicylic acid was used as the example of an exogenous acid which is transported out of the brain.

## CHAPTER II

### TRANSPORT OF 5HIAA FROM THE BRAIN

#### Section 1: Introduction

As discussed in the conclusion of Chapter I, the objectives of the present investigation can be accomplished by studying acids that are normally found in the brain (endogenous acids) and acidic compounds which must enter the brain from the circulation (exogenous acids). This chapter will be concerned with that section of the investigation dealing with the transport of endogenous acids from the brain.

The endogenous acid chosen to pursue the study of the transport system was 5-hydroxyindoleacetic acid (5HIAA). This compound is uniquely suited for this type of study, since it readily leaves the brain but does not enter it from the blood to a significant extent (26, 21). Such a unidirectional movement is indicative of a transport system. Although 5HIAA is found in the circulation, it is unlikely that a significant amount of this enters the brain; therefore, 5HIAA found in the central nervous system must be produced there (20). The main source of this acid is from the catabolism of 5-hydroxytryptamine (5HT; serotonin). The metabolic sequence can be diagrammed as follows:



The enzyme monoamine oxidase (MAO) oxidatively deaminates serotonin to the aldehyde, 5-hydroxyindoleacetaldehyde (5HIA),

which is further oxidized by an aldehyde dehydrogenase (AD) to the acid, 5HIAA. The 5HIAA once present, does not appear to leave the brain to any significant extent by passive diffusion. Although the arguments supportive of this conclusion have been presented in Chapter I, the importance of this concept warrants some repetition.

The administration of a monoamine oxidase inhibitor to rats blocks the synthesis of 5HIAA, producing a drop in the brain 5HIAA levels (19). If an inhibitor of acid transport is administered concomitantly with a monoamine oxidase inhibitor, the levels of 5HIAA remain unchanged (19). Any significant passive diffusion would have produced a fall in the 5HIAA brain concentration despite the transport inhibition. Furthermore, the lack of diffusion of 5HIAA into the brain from the blood (26, 21) would denote an equally deficient passive diffusion out of the brain. Yet, when the monoamine oxidase inhibitor pargyline was administered alone, the fractional turnover rate of 5HIAA was 85% per hour, indicating a very rapid exit of 5HIAA from the brain (20). It would be difficult to envision any other process besides transport as an explanation for the observations above.

Further evidence of the occurrence of transport of 5HIAA can be seen in studies where accumulation of the acid has resulted in the brains of animals treated with probenecid (18-20, 22, 23, 24). This blockade of transport is not unique to probenecid; phenylacetic acid and benzoic acid also produce an accumulation of 5HIAA (20, 25). This non-specificity

of inhibition leads to the hypothesis that the transport system is not specific to 5HIAA; that is, other acids besides 5HIAA can be transported by the system. If this be the case, it is possible that the inhibition of 5HIAA elimination produced by probenecid, phenylacetic acid, and benzoic acid results from the inhibitors' occupying a hypothetical carrier which is involved in the transport of 5HIAA from the brain. When the exogenous acids displace 5HIAA from the carrier, inhibition of 5HIAA brain transport results. It is probable that once these inhibitors occupy the carrier, they too are transported out of the brain. Although speculative, it appears reasonable that the brain should utilize the same or a similar system to rid itself of unwanted endogenous and exogenous organic acids as does the kidney.

The available evidence suggests that a relatively simple model can be developed to quantitate the transport of 5HIAA and to predict the levels of the acid following the administration of a transport inhibitor. If a model based on carrier kinetics were to fit the experimental data, it would constitute substantiation in vivo of the elimination of 5HIAA by a transport system.

## Section 2: Theoretical

The elimination of 5HIAA by a carrier mediated transport system may be described by an equation analogous to the Michealis-Menten equation for enzyme kinetics:

$$v = \frac{V_{\max} C_A}{K_m + C_A} \quad (1)$$

where  $v$  is the rate of transport of 5HIAA out of the brain;  $C_A$  is the concentration of 5HIAA in the brain;  $V_{\max}$  is the maximal rate of transport possible, and  $K_m$  is the concentration of 5HIAA in the brain that will produce half the maximal velocity. If a competitive inhibitor of the transport is present, then the equation for the rate of transport takes the form:

$$v_I = \frac{V_{\max} C_A}{K_m \left(1 + \frac{C_I}{K_I}\right) + C_A} \quad (2)$$

This equation is also borrowed from enzyme kinetics;  $v_I$  represents the rate of transport of 5HIAA from the brain in the presence of an inhibitor with concentration  $C_I$ ;  $K_I$  is the constant of inhibition. Equations 1 and 2 may be simplified, if  $K_m$  can be shown to be much larger than  $C_A$ . After the inactivation of monoamine oxidase, Tozer, et al. (18) noted that the rate of decline of 5HIAA was proportional to its concentration. This implied that

$$v = \frac{V_{\max}}{K_m} C_A \quad (3)$$

which would follow from Equation 1 if  $K_m$  is larger than  $C_A$ . Assuming that the presence of a transport inhibitor does not raise the levels of 5HIAA to a value approaching  $K_m$ , Equation 2 simplifies to

$$v_I = \frac{V_{\max} C_A}{K_m \left(1 + \frac{C_I}{K_I}\right)} \quad (4)$$

The assumptions leading to Equation 4 are somewhat justified

from a study by Tozer, et al. (18). After the administration of reserpine the levels of 5HIAA rose to a concentration more than twice the normal value. When the monoamine oxidase inhibitor, pargyline, was administered, the levels of 5HIAA declined in a monoexponential fashion, thus asserting that the rate of transport of 5HIAA was still proportional to the 5HIAA concentration despite the higher levels of the acid.

The steady state concentration of 5HIAA is primarily determined by two processes, the rate of synthesis from serotonin and other sources and the elimination of 5HIAA from the brain. Since diffusion of 5HIAA out of the brain appears to play an insignificant role, it will be assumed that this compound can only leave the brain through transport. The change of 5HIAA levels at steady state may then be described by the following:

$$\frac{dA}{dt} = R_{\text{syn}} - v = 0 \quad (5)$$

where  $\frac{dA}{dt}$  represents the change in the amount of 5HIAA in the brain with respect to time,  $R_{\text{syn}}$  is the rate of synthesis, and  $v$  is the rate of transport. Since at steady state the levels of 5HIAA in the brain are unchanged,  $\frac{dA}{dt} = 0$ . Assuming that the rate of synthesis does not change in the presence of a transport inhibitor, the change in the levels of 5HIAA in the brain after an inhibitor may be described by substituting Equation 4 into Equation 5, that is, replacing  $v$  with the rate of transport when an inhibitor is present,  $v_I$ . The result is

$$\left(\frac{dA}{dt}\right)_I = R_{\text{syn}} - \frac{V_{\text{max}} C_A}{K_m \left(1 + \frac{C_I}{K_I}\right)} \quad (6)$$

For the sake of further simplification, the constant  $k$  will be used in place of  $\frac{V_{\max}}{K_m}$  and will be referred to as a transport rate constant for 5HIAA. Substituting  $k$  into Equation 6 yields

$$\left(\frac{dA}{dt}\right)_I = R_{\text{syn}} - \frac{kC_A}{1 + \frac{C_I}{K_I}} \quad (7)$$

Equation 7 may be solved if it is known how the concentration,  $C_I$ , varies with time. If an inhibitor is used such that its elimination from the brain is monoexponential, the following equation would express how  $C_I$  varies with time:

$$C_I = C_{I_0} e^{-k_I t} \quad (8)$$

$C_{I_0}$  is the concentration of inhibitor in the brain at zero time and is a value obtained by extrapolation;  $k_I$  is the rate constant for elimination of the inhibitor. Using Equation 8 to substitute for  $C_I$  in Equation 7 produces the relationship

$$\left(\frac{dA}{dt}\right)_I = R_{\text{syn}} - \frac{kC_A}{1 + \frac{C_{I_0} e^{-k_I t}}{K_I}} \quad (9)$$

Equation 9 represents the model which describes the variation in 5HIAA concentration in the brain when an inhibitor which competes with 5HIAA for the carrier is present. It is important to note that for this equation to apply, the inhibitor's rate of decline must be proportional to the inhibitor concentration in the brain. Otherwise, a different function would have to be substituted for  $C_I$  in Equation 7. The use of the model will be discussed in Section 4 of this chapter (Results and Discussion). At this time it should be pointed



out that all the terms in Equation 9 can be independently determined with the exception of  $K_I$ , the inhibition constant; that is, the model is not necessary to ascertain the other terms. By solving Equation 9 with an analog computer (refer to Appendix A for computer diagram)  $K_I$  may be determined. Varying the value of  $K_I$  in the computer program generates different curves showing the change in brain 5HIAA levels with time following a dose of an inhibitor. The curve which is found to best fit the experimental data will correspond to the correct value for  $K_I$ . In this fashion it is possible to determine the brain concentration of an inhibitor which produces 50% inhibition, which by definition is  $K_I$ . The uniqueness of this technique is that only one dose is required and the  $K_I$  determined is not dependent on the time of sacrifice. Thus the classical log dose-response curve in which several doses are administered and the animals are all sacrificed at the same time can be avoided. An alternate method which does not require an analog computer to calculate  $K_I$  will be presented in the Results and Discussion section of this chapter.

The log dose-response curve, albeit useful, has the inherent disadvantage of being dependent on the time of sacrifice. Neff, et al. (19) report such a curve for the inhibition of 5HIAA transport out of the brain by probenecid. The accumulation of 5HIAA in rat brains two hours after various doses of probenecid was measured, and it was concluded that the maximal effect was approached by a dose of 200 mg/kg. The maximum accumulation was two and one-half

times the normal levels, and the approximate inhibitor dose producing 50% inhibition was 20 mg/kg. The present investigation, however, has shown that the accumulation of 5HIAA is very dependent on time, as would be expected since the inhibitor levels in the brain are not constant with time. The time dependency of 5HIAA accumulation after a 100 mg/kg dose of probenecid may be seen in Figure 2-1. The experiment leading to these data will be discussed in detail below. At this time the intent is solely to show that the levels of 5HIAA rise after a dose of inhibitor, reach a maximum, and then decline with time. In the study depicted by Figure 2-1, 24 hours after the dose of probenecid the concentration of 5HIAA in the brain had returned to normal. The major idea to be gained from Figure 2-1 is that the time of sacrifice of the animals determines how high an accumulation of 5HIAA will be seen. In this study the maximum accumulation occurs between one and two hours; however, with a higher or lower dose of probenecid this may no longer be the time of maximum accumulation. In a classical log dose-response study such as the one reported by Neff, et al. (19), the interpretations could be erroneous if the time of sacrifice were too early, for then the maximum accumulation would never be seen. Furthermore, the magnitude of the inhibitor dose producing 50% inhibition would vary depending on the time of sacrifice. It is proposed in the present investigation that the aforementioned problems may be avoided by using the model presented in Equation 9. The experimental procedure to be used in testing this model will be described below.

### Section 3: Experimental

Materials: All chemicals used were of analytical grade. Probenecid as the free acid was supplied by Merck Sharpe and Dohme, Inc., West Point, Pennsylvania. The following other materials were used: 5-hydroxyindoleacetic acid, (ethylenedinitrilo)tetraacetic acid disodium salt, monobasic and dibasic potassium phosphate, zinc sulfate, pepsin (N.F. Granular), Regisil<sup>®</sup>, gas chromatography glass column 6' x 1/8" packed with 3% OV-1<sup>®</sup> on High Performance Chromasorb W<sup>®</sup> 80/100 mesh, nitrogen gas (prepurified), oxygen (extra dry), hydrogen gas (prepurified), hydrochloric acid, sodium hydroxide, ether, heptane.

Animals: Male Sprague-Dawley rats weighing 190-210g were obtained from Horton Laboratories, Inc., Oakland, California, and used throughout this investigation. Earlier studies also reported utilized rats from Simonsen Laboratories, Gilroy, California.

Apparatus: Aminco-Bowman spectrophotofluorometer model 8210, Varian gas-liquid chromatography model 204-C, Tenbroeck tissue grinder, Vortex Jr. Mixer model K-500-J, Lab-Tek<sup>®</sup> Aliquot Mixer, International centrifuge model EXD, Mettler analytical balance type B6, Tektronix programmable calculator model Statistician 911, test tube heater model 100C from Hallikainen Instruments, Richmond, California, Dubnoff Metabolic Shaking Incubator, guillotine from the Harvard Apparatus Co., Inc., Millis, Massachusetts, 15 ml ground glass centrifuge tubes with stoppers (centrifuge tube),

20 ml screw cap culture tubes with teflon-lined caps (culture tube), assorted glassware and small equipment.

Experimental Design: Before each experiment involving the transport of 5HIAA the following solutions were freshly prepared:

1) Injection solution: Probenecid was chosen to inhibit the transport of 5HIAA. Depending on the dose required, the proper quantity of probenecid was weighed on an analytical balance and the powder quantitatively transferred to a volumetric flask. Since probenecid was used as the free acid, the drug was wetted with an equivalent amount of a 1N solution of sodium hydroxide. Enough distilled water was then added to dissolve the probenecid; then 10 ml of a pH 7 phosphate buffer was added. Enough distilled water was added to bring up the volume to 100 ml. For a dose of 100 mg/kg, a solution of 20 mg/ml of probenecid was prepared; rats weighing 200 g would then receive 1 ml of the injection solution. For other doses of probenecid, the concentration of probenecid in the injection solution was adjusted correspondingly.

2) 5HIAA standard solution: 10 mg of 5HIAA were weighed and dissolved in a volumetric flask with enough distilled water to make 100 ml of solution with a concentration of 100  $\mu\text{g/ml}$ . One ml of this solution was then transferred into a volumetric flask and the volume brought up to 100 ml using 0.1 N HCl resulting in a 1  $\mu\text{g/ml}$  solution of 5HIAA. These solutions were used in the preparation of standard curves for the spectrophotofluorometric assay of 5HIAA to be discussed later.

3) Phosphate buffer - pH 7: A 0.5 M solution of monobasic potassium phosphate was prepared by dissolving 34.02 g of the salt in sufficient water to make 500 ml of solution. A 0.5 M solution of dibasic potassium phosphate was prepared by similarly dissolving 43.545 g in water. Using these two solutions, a pH 7 buffer was prepared by adding enough of the first solution to the entire volume of the latter. The mixing was monitored with a pH meter to ascertain when a pH of 7 was reached.

4) (Ethylenedinitrilo)tetraacetic acid disodium salt solution (EDTA): To prepare a 0.05 M solution 930.6 mg of the salt was dissolved in enough water to make 50 ml of solution. This solution, which shall henceforth be referred to as EDTA, was used to prevent coagulation of whole blood.

5) Zinc sulfate solution: The monohydrate of zinc sulfate was used to prepare a 2.5% solution in distilled water.

6) Hydrochloric acid solutions: A 6 N and a 0.1 N solution of hydrochloric acid was prepared by diluting the appropriate volume of concentrated hydrochloric acid with distilled water.

The injection and sacrifice of animals was carried out once the solutions above were prepared. Groups of rats with five per group were randomly selected. A control group with eight rats was set aside from the others and received no treatment. The remaining rats all received one ml of the injection solution. (In one study the rats were administered a dose corresponding to 100 mg/kg; in another the dose was 300 mg/kg.) Since the intent was to sacrifice the rats at

different times after administering probenecid to them, an injection schedule was arranged so that the last group to be sacrificed was injected first; the first group to be sacrificed was injected last. Also, the injections of the individual rats in each group were staggered by two minutes so that at the time of sacrifice all rats in the same group would have the same time elapsed from the time of injection. After the appropriate interval, each group of rats was sacrificed by decapitation. Whole blood was collected in 50 ml beakers containing 200  $\mu$ l of EDTA solution to prevent coagulations of the blood. After mixing the blood with the EDTA by rotating the beaker, it was quickly transferred to a centrifuge tube. The sample was numbered and set aside. The next step was the rapid extirpation of the brain from the decapitated head, taking care to blot with an absorbent tissue excess blood from the surface of the brain. At the same time the larger blood vessels of the pia mater were removed. The brain with a minimum of spinal cord was then wrapped in a small section of aluminum foil, numbered, and put into ground dry ice. The time elapsed from the decapitation to the freezing of the brain rarely exceeded one minute. The entire procedure was repeated for each rat in a group. Upon completion of an entire time group, all the collected blood samples were centrifuged for approximately five minutes to separate the plasma.

After centrifugation, 1 ml from each plasma sample was transferred into a correspondingly numbered culture tube.

These samples were rapidly frozen and stored for analysis of their probenecid content at a later time; control plasmas were pooled and also stored frozen.

Due to the instability of 5HIAA in a neutral or basic medium, it was highly desirable to homogenize the brains as soon as possible, and to stabilize the 5HIAA by acidifying the brain homogenate. The homogenization was, therefore, carried out on the same day as the sacrificing. Each brain was homogenized individually. First the brain was weighed while still frozen; then it was transferred to a Tenbroeck tissue grinder with a motor driven pestle. For each gram of rat brain, 3 ml of a chilled 0.1 N hydrochloric acid solution was pipetted into the tissue grinder, and the homogenization was then performed. The entire process would take about a minute per brain. After homogenization, 3 ml of homogenate, representing 0.75 g of brain, was transferred to a culture tube, labeled, and stored for the analysis of probenecid. With homogenization the initial phase of the study was complete. The analysis of brain 5HIAA concentration was always postponed until the following day, due to the length of time involved in the first part of the experiment.

5HIAA Analysis: The fluorometric assay of Udenfriend, et al. (27) was used with the modifications described below. A standard curve using known concentrations of 5HIAA was prepared at the same time that brain levels of 5HIAA were to be determined. The stock solutions of 5HIAA described above were used for this purpose. Varying volumes of the stock

solutions were pipetted into culture tubes to prepare samples containing different amounts of 5HIAA. All samples were then brought up to 1 ml with 0.1 N hydrochloric acid. An aliquot of 3 ml of 0.1 N hydrochloric acid was then added to each sample and the sample agitated using a vortex mixer. Three ml of each sample was then transferred into culture tubes. The purpose of this final step was to simulate the transferring of 3 ml of brain homogenate for the 5HIAA analysis. Three control samples were also prepared by pipetting 3 ml of 0.1 N hydrochloric acid into culture tubes. The following extraction procedure was then used for the standards and the brain samples.

- 1) To culture tubes containing 3 ml of brain homogenate or 3 ml of standard 5HIAA solution add 4 ml of a 2.5% zinc sulfate solution.
- 2) Add 0.5 ml of a 1 N sodium hydroxide solution and stir each sample immediately using a vortex mixer.
- 3) Centrifuge the samples at a medium setting (approximately 1400xg) for 5 minutes.
- 4) Transfer 4 ml of the supernate into centrifuge tubes containing approximately 2 g of sodium chloride and 0.3 ml of a 6 N solution of hydrochloric acid.
- 5) Add 5 ml of anhydrous ether to each sample; stopper with ground glass stoppers, then shake each sample gently by hand for ten seconds. After all samples are shaken, repeat the shaking procedure for five seconds. The shaking must be gentle to avoid emulsification of the samples. Some emulsion invariably forms, but this separates upon centrifugation.
- 6) Centrifuge as in step 3) above, then transfer 4 ml of the ether phase into centrifuge tubes containing 2 ml of a pH 7, 0.5 M phosphate buffer.
- 7) Shake vigorously for fifteen seconds and centrifuge again.



- 8) Using a disposable Pasteur pipette and Propipette<sup>®</sup>, transfer most of the buffer phase into a quartz cuvette and read the fluorescence of the sample at the maximum activation and fluorescence wavelengths for 5HIAA. The uncorrected wavelengths used for maximum activation and fluorescence were 315 and 370 nm, respectively; the actual activating and fluorescence wavelengths for 5HIAA are 295 and 340 nm.

The following precautions should be observed when performing this assay to insure good results. The glassware must be meticulously cleaned and rinsed with glass distilled water. Screw cap glassware should not be used in the presence of organic solvents to avoid fluorescence contamination. Furthermore, it was found that sodium chloride produced a strong fluorescence peak at 420 nm which interfered with the 5HIAA fluorescence. Reagent grade sodium chloride was found to be free of this contamination. Chemicals stored in plastic should be avoided; for example, concentrated hydrochloric acid packaged in plastic bottles was found to produce a higher fluorescence blank than hydrochloric acid from glass bottles.

An example of a fluorescence standard curve may be seen in Figure 2-2. Since the extraction procedure was identical and carried out at the same time for both standards and brain samples, it was possible to convert fluorescence readings from the brain samples directly into micrograms of 5HIAA per gram of brain weight. To accomplish this, the points on the standard curve were fitted to a straight line by the method of least squares, and the parameters of this line were then used to calculate concentration units from fluorescence units.

Plasma Probenecid Analysis: At the inception of this investigation, the only assay reported for probenecid was that of Dayton, et al. (28), which utilized a spectrophotometric method. This assay was found to be unsatisfactory if the levels of probenecid in the plasma fell below 10 µg/ml. Furthermore, when this assay was used for the quantitation of probenecid in brain it was found to be totally unsuitable. It was necessary, therefore, to develop an entirely new assay in an effort to increase the sensitivity and the specificity. Because of the inherent ability of gas-liquid chromatography (GLC) to quantitate and separate an unknown substance from its components, it was decided to use this instrumentation to develop an analytical procedure for probenecid in biological tissues.

Probenecid is too polar a compound to be chromatographed without derivatization. The trimethylsilyl ester of probenecid, on the other hand, was found to give sharp peaks with reasonable retention times using a flame ionization detector with a hydrogen and oxygen flame and nitrogen as a carrier gas. Different liquid phases were tried with a High Performance Chromasorb W<sup>®</sup> 80/100 mesh as the solid support in a stainless steel 6' x 1/8" column. The best resolution was obtained using a support with 3% OV-1<sup>®</sup>, a nonpolar phase described by the manufacturer as a methylsilicone polymer. Standard curves were prepared using known concentrations of probenecid which had been silylated for two hours with 100 µl of bis(trimethylsilyl)trifluoroacetamide, Regisil<sup>®</sup>.

The standard curves, however, were not satisfactory, since they had a positive x-intercept; that is, they did not cross through zero. Since this is indicative of nonlinearity at the lower concentrations, it was suspected that there was excessive adsorption of the silyl ester of probenecid on the column. The metal column was then replaced with a pyrex column, and the linearity was greatly improved. Although the curve still had a positive x-intercept, it was possible to obtain acceptable standard curves. The methyl ester of probenecid was synthesized by Fisher esterification with methanol and used as an internal standard when preparing standard curves. Figure 2-3 is an example of a standard curve for probenecid extracted from control plasmas. The abscissa is the concentration of probenecid per milliliter of plasma while the ordinate is the ratio of the height of the probenecid peak to the height of the internal standard peak. This ratio is normally referred to as the peak height ratio (P.H.R.).

The procedure for preparing a standard curve for probenecid extracted from plasma is given below. The same extraction procedure was used for plasma samples in a transport study.

- 1) To 1 ml of control plasma samples, add varying microliter volumes of stock solutions of probenecid in phosphate buffer. Mix repeatedly on a Vortex mixer to insure intimate mixing of the probenecid in the plasma.
- 2) Add 1 ml of a 5 mg/ml solution of pepsin in water to all samples.

- 3) Add 2 ml of 0.1 N hydrochloric acid to all samples; mix on Vortex, and store for 3 hours at approximately 50°C to allow digestion of the plasma proteins by the pepsin.
- 4) At the end of the digestion period allow samples to come to room temperature, then add 5 ml of anhydrous ether. Shake for 10 minutes on a Lab-Tek<sup>®</sup> mixer and centrifuge for 5 minutes to separate the phases.
- 5) Transfer 4 ml of ether from above into a culture tube with 5 ml of a 0.1 M solution of dibasic potassium phosphate. Shake and centrifuge as above.
- 6) Transfer 4 ml of phosphate layer into a culture tube with 1 ml of 6 N hydrochloric acid.
- 7) Add 5 ml of ether to each sample. Shake and centrifuge as above.
- 8) After centrifugation transfer 4 ml of ether phase into a centrifuge tube containing a known amount of the internal standard (methyl probenecid) in ether.
- 9) Evaporate the ether to dryness on a test tube heater then react with 100  $\mu$ l of Regisil<sup>®</sup> for 2 hours.
- 10) Using a Hamilton 10  $\mu$ l syringe, inject 1-2  $\mu$ l samples into the gas-liquid chromatograph.

Figure 2-4 is a typical GLC recording for probenecid extracted from plasma. Gas flow rates and instrument temperatures are listed in Figure 2-4. It should be pointed out that to optimize the accuracy of this procedure, a standard curve should be prepared on the day before analyzing unknown samples. Pepsin digestion of the plasma proteins was found to be desirable before extraction to allow complete recovery of the probenecid from the plasma. Also, because of the nonlinearity of the standard curves over a wide concentration range, it was better to prepare two or more standard curves

rather than just one. For example, a standard curve with a concentration range of 2-10  $\mu\text{g}$  of probenecid was prepared using 3  $\mu\text{g}$  of internal standard, and another one with a range of 20-200  $\mu\text{g}$  of probenecid was prepared using 30  $\mu\text{g}$  of internal standard. This resulted in a better standard curve than if the range 2-200  $\mu\text{g}$  had been used. Since a large amount of surplus plasma was obtained from each sacrificed rat, it was possible to pool plasma samples from each time group for preliminary assays to determine the concentration ranges which should be used in the standard curves.

Brain Probenecid Analysis: The assay for brain probenecid, although basically the same as that described above for plasma, was complicated by the low concentrations of probenecid and the high levels of contaminants which extracted along with the probenecid. As an organic solvent, a mixture of equal volumes of ether and n-heptane was found to be preferable to ether alone, since less contaminants were extracted from the brain homogenate when the mixed-solvent system was used. Prolonged shaking of the samples was also found to be necessary to extract all of the probenecid from the homogenate. Digestion of the brain homogenate with pepsin as with plasma samples did not produce satisfactory results. A double extraction reduced the contaminants to an acceptable level. The extraction procedure is given below:

- 1) Add 2 g of sodium chloride and 0.3 ml of 6 N hydrochloric acid to each brain homogenate sample. Mix on Vortex.
- 2) Add 5 ml of a mixture of equal volumes of ether and n-heptane.

- 3) Shake samples gently on a Lab-Tek<sup>®</sup> mixer for 30 minutes, then centrifuge for 5 minutes at a medium speed.
- 4) Transfer 4 ml of the organic phase into a culture tube containing 5 ml of a 0.1 M solution of dibasic potassium phosphate.
- 5) Shake for 15 minutes on a Lab-Tek<sup>®</sup> mixer and centrifuge as above.
- 6) Carefully transfer 4 ml of the phosphate layer into another culture tube with 1 ml of 6 N hydrochloric acid. Since the lower layer has to be separated in this step, it becomes necessary to use care to avoid mixing of the two phases. This separation may be accomplished using a volumetric 4 ml pipette and a Propipette<sup>®</sup>.
- 7) Add 5 ml of ether and shake for 15 minutes as in step 5 above. Centrifuge.
- 8) Transfer 4 ml of ether phase into a centrifuge tube containing a known amount of internal standard in an ether solution.
- 9) Evaporate the ether to dryness, then react with 50  $\mu$ l of Regisil<sup>®</sup> for 2 hours.
- 10) Using a Hamilton 10  $\mu$ l syringe, inject 1-2  $\mu$ l samples onto the gas-liquid chromatographic column.

To prepare a standard curve, the same extraction procedure as described above was used to assay known concentrations of probenecid in control brain homogenates. These standard samples were prepared by adding varying  $\mu$ l volumes of stock solutions of probenecid in phosphate buffer to 3 ml samples of brain homogenate. Microliter volumes were used when adding the probenecid to the homogenates in order to avoid large dilutions of the homogenates. The samples were mixed repeatedly on a Vortex mixer to insure complete dispersion of the probenecid in the standard sample. The remaining procedure was as described above. Figure 2-5 is a typical

GLC recording of probenecid extracted from brain samples. The standard curves obtained from brain samples were similar to those obtained in the plasma assays.

#### Section 4: Results and Discussion

The concentrations of 5HIAA assayed in rat brains after doses of 100 and 300 mg/kg of probenecid are listed in Table I along with the corresponding times of sacrifice. Also included are unpublished data of Tozer, et al. (29) for an experiment in which rats received 100 mg/kg of probenecid intraperitoneally. The latter data preceded the results of the present investigation by five years; however, they have been included for comparison. The results from this early experiment shall henceforth be referred to as Tozer's data. The values reported in Table I are the arithmetic means of five brain samples and the corresponding standard errors. The control levels of 5HIAA were obtained from the brains of ten rats which had not received any probenecid.

The results of the assays for plasma and brain probenecid as performed in this study are reported in Tables II and III. It will be noted that rather than listing the arithmetic mean of five animals, for each time point, geometric means have been calculated. The reason for this being that the probenecid data was graphed on semi-logarithmic plots. Also listed in Tables II and III are the logarithms of the geometric means and their corresponding standard errors. Table IV lists the plasma concentrations obtained by Tozer (29) after the intraperitoneal administration of 100 and 200

TABLE I  
 RAT BRAIN 5HIAA CONCENTRATIONS AFTER INTRAPERITONEAL  
 DOSES OF PROBENECID

Time of Sacrifice (Hrs)	Brain Concentrations ( $\mu\text{g/g}$ ) *		
	100 mg/kg Dose	100 mg/kg** Dose	300 mg/kg Dose
0	.37 $\pm$ .01	.25 $\pm$ .03	.30 $\pm$ .01
.4†	.41 $\pm$ .03		
.5		.38 $\pm$ .02	.44 $\pm$ .02
1.0	.56 $\pm$ .04	.46 $\pm$ .03	.59 $\pm$ .01
2.0	.56 $\pm$ .02	.50 $\pm$ .01	.78 $\pm$ .05
3.0	.50 $\pm$ .01	.47 $\pm$ .02	.95 $\pm$ .04
4.0	.51 $\pm$ .01	.54 $\pm$ .01	1.02 $\pm$ .06
5.0	.45 $\pm$ .02	.41 $\pm$ .03	1.12 $\pm$ .04
6.0	.43 $\pm$ .02	.42 $\pm$ .04	.98 $\pm$ .04
8.0			.88 $\pm$ .05
24.0	.37 $\pm$ .02		

\* Mean of five animals  $\pm$  Standard Error.

\*\* Data from Tozer et al. (29).

† The animals were sacrificed mistakenly at 0.4 hrs rather than 0.5 hrs.



TABLE II

## RAT PLASMA AND BRAIN PROBENECID LEVELS AFTER A 100 mg/kg INTRAPERITONEAL DOSE OF PROBENECID

Time of Sacrifice (hrs)	Plasma Concentration ( $\mu\text{g/ml}$ )*	Log Plasma Concentration $\pm$ S.E.	Brain Concentration ( $\mu\text{g/g}$ )*	Log Brain Concentration $\pm$ S.E.
0	0		0	
0.4	274.85	2.4391 $\pm$ .0170	13.74	1.1380 $\pm$ .0264
1.0	222.33	2.3470 $\pm$ .0170	15.42	1.1881 $\pm$ .0168
2.0	80.72	1.9070 $\pm$ .0318	8.08	0.9074 $\pm$ .0825
3.0	34.79	1.5414 $\pm$ .1380	1.12	0.0492 $\pm$ .0372
4.0	7.55	0.8779 $\pm$ .0316	No detectable probenecid	
5.0	2.37	0.3747 $\pm$ .1503		
6.0	1.98	0.2967 $\pm$ .0612		
24.0	0			

\* Geometric mean of five animals.

TABLE III

RAT PLASMA AND BRAIN PROBENECID LEVELS AFTER A 300 mg/kg INTRAPERITONEAL DOSE OF PROBENECID

Time of Sacrifice (hrs)	Plasma Concentration ( $\mu\text{g/ml}$ )*	Log Plasma Concentration $\pm$ S.E.	Brain Concentration ( $\mu\text{g/g}$ )*	Log Brain Concentration $\pm$ S.E.
0	0		0	
0.5	666.32	2.8237 $\pm$ .0100	68.98	1.8387 $\pm$ .0144
1.0	599.98	2.7781 $\pm$ .0155	97.60	1.9894 $\pm$ .0272
2.0	498.87	2.6980 $\pm$ .0176	89.49	1.9540 $\pm$ .0284
3.0	438.67	2.6421 $\pm$ .0256	66.50	1.8228 $\pm$ .0219
4.0	339.02	2.5302 $\pm$ .0190	52.40	1.7193 $\pm$ .0496
5.0	232.02	2.3655 $\pm$ .0533	33.57	1.5260 $\pm$ .0695
6.0	172.50	2.2368 $\pm$ .0651	22.71	1.3562 $\pm$ .0654
8.0	109.79	2.0406 $\pm$ .0887	11.84	1.0734 $\pm$ .1067

\* Geometric mean of five animals.

TABLE IV  
 RAT PLASMA PROBENECID CONCENTRATIONS AFTER 100 AND 200 mg/kg INTRAPERITONEAL  
 DOSES OF PROBENECID

Time of Sac- rifice (hrs)	Plasma Concentrations		
	200 mg/kg Dose	Log Plasma Con- centration + S.E.	100 mg/kg Dose
0	0		0
0.5	420.4	2.624 ± .045	289.8
1.0	315.7	2.499 ± .056	230.8
2.0	278.3	2.444 ± .030	137.9
3.0	230.4	2.362 ± .009	43.4
4.0	128.8	2.110 ± .030	26.0
5.0	87.7	1.943 ± .045	8.8
6.0	50.1	1.700 ± .134	5.7
			Log Plasma Con- centration + S.E.
			2.462 ± .014
			2.363 ± .016
			2.139 ± .010
			1.637 ± .134
			1.415 ± .205
			0.944 ± .197
			0.756 ± .203

\* Data from Tozer, et al. (29).

mg/kg doses of probenecid to rats. Figures 2-6, 2-7, and 2-8 are graphical representations of the data contained in Tables II, III, and IV. It should be reemphasized that these figures are semi-logarithmic plots of probenecid concentrations versus time. The linearity of these plots indicates that the elimination of probenecid involves an apparent first order process; thus it is possible to determine the half life of elimination for probenecid from the slopes of these figures. The calculated half life values for the different studies are given in Table V. Apparently the elimination half life of

TABLE V  
PROBENECID HALF LIVES AFTER DIFFERENT DOSES

Dose (mg/kg)	Half-life (hrs)
100*	0.9
100	0.7
200*	1.9
300	2.6

\* Data from Tozer, et al. (29).

probenecid increases as the dose increases. This has been previously reported by Dayton (28) in humans, and this present study verifies those results.

The use of probenecid in this study, as mentioned in the introduction, was primarily for its ability to block or

inhibit acid transport systems. This being the case, the dose-dependence of probenecid's elimination kinetics does not invalidate its use for the aforementioned purpose. On the contrary, if it should continue to block 5HIAA elimination from the brain despite different probenecid doses and different half lives of elimination, it could possibly serve to verify the existence of a transport system to eliminate acids from the brain. The logic being that if 5HIAA levels accumulate in the presence of probenecid and since probenecid is an acidic compound known to inhibit other physiological acid transport systems, the possibility exists that 5HIAA is also eliminated from the brain by an acid transport system. Other arguments to support this premise have been previously presented in Chapter I. If higher doses of probenecid with longer half lives of elimination produced higher accumulation of 5HIAA this could further lend credibility to the existence of a transport system for 5HIAA elimination from the brain.

Figure 2-1, which has been previously presented, is a graph of the data from Table I obtained after administering 100 mg/kg of probenecid to rats and monitoring the brain levels of 5HIAA for 24 hours. The concentration of 5HIAA was seen to increase, reach a maximum in 1-2 hours, then gradually decrease toward the control concentration levels. As may be seen in Figure 2-1, the 24-hour group, that is, the rats sacrificed 24 hours after probenecid treatment, had a brain concentration of 5HIAA identical to the control level. By reference to Figure 2-6, it can be seen that the probenecid brain levels underwent a similar fluctuation over this

same period of time. This fluctuation of probenecid levels could account for the rise and fall in the 5HIAA levels. Probenecid, however, is eliminated by first order kinetics, and thus the amount of probenecid at any time can be readily expressed by Equation 8 as discussed in Section 2. This facilitated the use of the model expressed in Equation 9. The goal then, at this point, was to convert the kinetic model into a computer diagram and thereby utilize an analog computer to generate 5HIAA brain concentration-time curves. The diagram utilized is explained in Appendix A. It should be emphasized at this point that the model as previously developed assumes the presence of a competitive inhibitor and the existence of a transport system for 5HIAA. Thus, if the model has validity, an analog computer should be capable of generating 5HIAA brain concentration-time curves similar to those obtained experimentally. Figure 2-9 is the same data as in Figure 2-1 with the brain levels of 5HIAA expressed as a percent of the control levels. The brain levels of 5HIAA are expressed as a percent of the control levels for the particular study. Normalization of the 5HIAA levels served to facilitate the generation of curves by the computer. The curve traced over the points in Figure 2-9 was generated by an analog computer utilizing the model as mentioned. Furthermore, the computer fit was repeated utilizing Tozer's 5HIAA data (29), and the results can be seen in Figure 2-10. The results of the computer fit of the 5HIAA data obtained after a 300 mg/kg dose of probenecid may be seen in Figure 2-11. The curve which was found to best fit the in vivo

data was taken to represent the one in which the proper  $K_I$  had been utilized. In this manner the constant of inhibition was calculated from the best computer fit of the brain 5HIAA data. Another way to express the use of the computer is to state that the model or the differential equation was solved by the computer by generating a curve which best fit the data. The constants of inhibition calculated by computer fit of the 5HIAA data are given in Table VI. Further discussion on the use of the analog computer may be found in Appendix A.

TABLE VI  
CONSTANTS OF INHIBITION ( $K_I$ 'S) CALCULATED FROM  
COMPUTER FITS OF 5HIAA DATA

Probenecid Dose (mg/kg)	Probenecid Half Life (hrs)	$K_I$ ( $\mu\text{g/ml}$ )
100	0.7	52
100*	0.9	55
300	2.6	58

\* Data from Tozer et al. (29).

As can be seen, the values listed in Table VI are similar despite large differences in the time at which the 100 mg/kg studies were carried out (1967 and 1972), a three-fold increase in the probenecid dose, and a large change in the elimination half life of probenecid. From this table it is apparent that the different half lives of probenecid elimination had little if any effect on the estimate of  $K_I$ ,

although the effect on the 5HIAA levels was markedly different as may be seen by comparing Figures 2-9 and 2-11. The latter difference is to be expected if a transport system exists, for the longer the inhibitor is present, the more the 5HIAA would be expected to accumulate.

In an attempt to verify the magnitude of the  $K_I$  values obtained using the computer fit of the in vivo data, calculation of the constant of inhibition by another method was undertaken. Since by definition  $K_I$  is the concentration of inhibitor which produces a 50 percent inhibition of transport, a plot of the percent inhibition against the logarithm of the inhibitor concentration should give an estimate of  $K_I$ . This plot is analogous to a response-logarithm dose plot. The percent inhibition was calculated from the rates of transport of 5HIAA from the brain in the presence and absence of the inhibitor as follows:

$$\% \text{ Inhibition} = \left( \frac{v - v_I}{v} \right) \times 100 \quad (10)$$

where  $v$  is the rate of 5HIAA transport when no inhibitor is present, that is, the normal elimination rate of 5HIAA from the brain. The rate of 5HIAA transport in the presence of the inhibitor is represented by  $v_I$ . As discussed in Section 2 of this chapter, the rate of change in the amount of 5HIAA,  $\frac{dA}{dt}$ , in the brain is dependent on the synthesis rate,  $R_{\text{syn}}$ , as well as the rate of elimination or the 5HIAA transport rate,  $v$ . This may be represented in equation form as:

$$\frac{dA}{dt} = R_{\text{syn}} - v \quad (11)$$



Thus, the rate of transport can be expressed as follows:

$$v = R_{\text{syn}} - \frac{dA}{dt} \quad (12)$$

When no transport inhibitor is present the levels of 5HIAA should not fluctuate within the time of measurement, that is,  $\frac{dA}{dt} \cong 0$ . Thus when 5HIAA is at a steady state the rate of transport will be equal to the rate of synthesis. In the presence of probenecid, however, the levels of 5HIAA will fluctuate from the steady state and the  $v_I$  can be determined as follows:

$$v_I = R_{\text{syn}} - \frac{\Delta A}{\Delta t} \quad (13)$$

where  $\frac{\Delta A}{\Delta t}$  is an estimate of  $\frac{dA}{dt}$  and represents the experimental change in the amount of 5HIAA over an interval of time. Since 5HIAA levels will rise in the presence of a transport inhibitor, the rate of transport that would be expected if no inhibitor were present would have to be higher than the rate of synthesis. As previously mentioned, the rate of 5HIAA transport has been shown by Tozer, et al. (18) to be proportional to the levels of 5HIAA. Thus the following expression for  $v$  may be written:

$$v = k\bar{A} \quad (14)$$

where  $\bar{A}$  represents the mean value of 5HIAA in an interval of time  $\Delta t$ . Substituting the latter two equations into the expression for the percent of inhibition, Equation 10, results in the following:

$$\% \text{ Inhibition} = \left( \frac{k\bar{A} - R_{\text{syn}} + \frac{\Delta A}{\Delta t}}{k\bar{A}} \right) 100 \quad (15)$$

or expressed in terms of concentration,

$$\% \text{ Inhibition} = \left( \frac{k\bar{C}_A - \frac{R_{\text{syn}}}{v_B} + \frac{\Delta C_A}{\Delta t}}{k\bar{C}_A} \right) \times 100 \quad (16)$$

where  $v_B$  is the volume of the brain.

Thus the percent inhibition may be determined at different time intervals from the plot of brain levels of 5HIAA with time by simply determining the change in 5HIAA concentration ( $\Delta C_A$ ) for each time interval ( $\Delta t$ ). The mean value for the 5HIAA concentration ( $\bar{C}_A$ ) was calculated by taking the sum of the concentrations of 5HIAA at the beginning and end of each time interval and dividing by two. Thus the value used for  $\bar{C}_A$  was an estimate of what the concentration of 5HIAA was in the brain at the midpoint of a time interval. Table VII contains the percent inhibition values obtained for different time intervals when probenecid was administered. The next step in the process of calculating  $K_I$  from the percent inhibition is to plot the percent inhibition versus the logarithm of the inhibitor concentration in the brain or in the plasma which produced the inhibition. These latter values were obtained from the semi-logarithmic plots of the inhibitor levels versus time, i.e., Figures 2-6, 2-7, and 2-8. Since the brain concentrations of probenecid were not determined in one of the studies, it was decided to utilize the plasma concentrations of probenecid for the plot to estimate  $K_I$ . Since the percent inhibition values were determined for an interval of time, the average probenecid plasma

TABLE VII  
 CALCULATED PERCENT INHIBITION VALUES AFTER  
 INTRAPERITONEAL DOSES OF PROBENECID

$\Delta t$ (hrs)	100 mg/kg dose % Inhibition	100 mg/kg dose* % Inhibition	300 mg/kg dose % Inhibition
0-.4	31		
0-.5		110	96
.5-1		77	102
.4-1	73		
1-2	35	59	84
2-3	18	42	85
3-4	28	65	77
4-5	11	18	82
5-6	12	42	59
6-8			63

\* Calculated using data from Tozer, et al. (29).

concentration during the time interval for which the percent inhibition was determined was needed. The plasma concentration at the midpoint of the time interval was used. Table VIII lists the calculated percent inhibition values for the three experiments and the corresponding plasma concentrations which existed at the midpoint of the time interval. It should be noted that this table is composed from the data of Tables II, III, IV, and VII. From the information on Table VIII the percent inhibition was plotted against the logarithm of the plasma concentration of probenecid, Figure 2-12. As may be seen from this figure 50 percent inhibition occurred when the plasma levels were about 80  $\mu\text{g}/\text{ml}$ . By comparing this value of  $K_I$  with the values obtained from the computer fits in Table VI, the correlation between the  $K_I$ 's calculated by the two different methods can be noted.

The curve drawn in Figure 2-12 is theoretical. The relationship between percent inhibition and the inhibitor concentration is derived by substituting Equation 7 in Equation 16:

$$\% \text{ Inhibition} = \frac{C_I}{K_I + C_I} \times 100 \quad (17)$$

The theoretical curve has the S-shape shown. It is placed in the figure where it appears to best approximate the data presented.

Although the  $K_I$  from Figure 2-12 results from a plot similar to a response-logarithm dose plot, the  $K_I$  determined by this method is independent of the time of sacrifice. In a normal dose-response ( $\text{ED}_{50}$ ) determination all animals must be

TABLE VIII  
PERCENT INHIBITION VALUES WITH CORRESPONDING  
PROBENECID PLASMA CONCENTRATIONS

% Inhibition	Probenecid Plasma Concentration ( $\mu\text{g/ml}$ )
11	5
12	2
18	17
18	58
28	21
31	137
35	151
42	7
42	91
59	202
59	184
63	141
65	35
73	248
77	260
77	389
82	286
84	549
85	469
96	333
102	633
110	145

sacrificed at the same time after being treated with a range of doses. After a single dose, the plasma levels of a drug are constantly changing with time. The time of sacrifice, therefore, has an effect on the  $ED_{50}$  value determined. The method tested in this report is not only time independent but can also be used to determine a  $K_T$  utilizing a single dose administered to a number of animals.

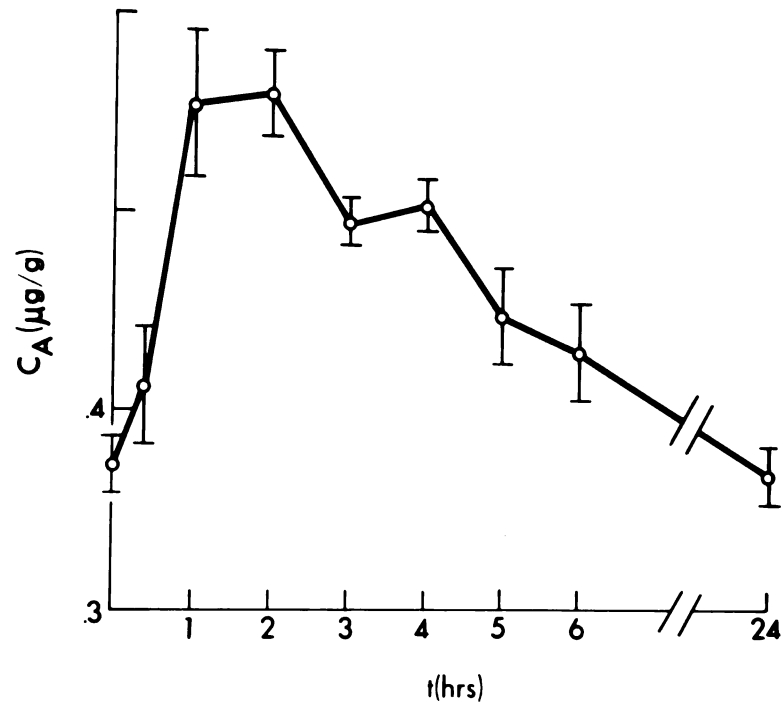


Figure 2-1. Rat brain 5HIAA concentrations after a 100 mg/kg intraperitoneal dose of probenecid. The concentration,  $C_A$ , is expressed in micrograms per gram of brain tissue.

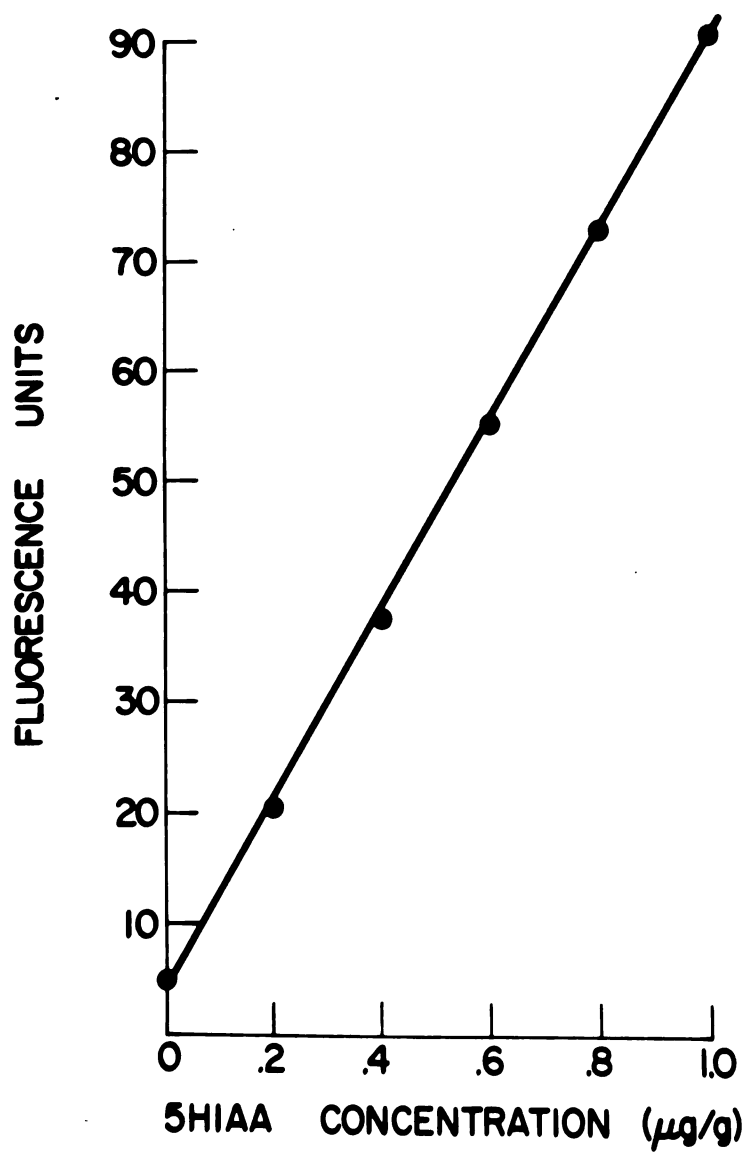


Figure 2-2. Standard curve for 5HIAA. The fluorescence units are arbitrary.



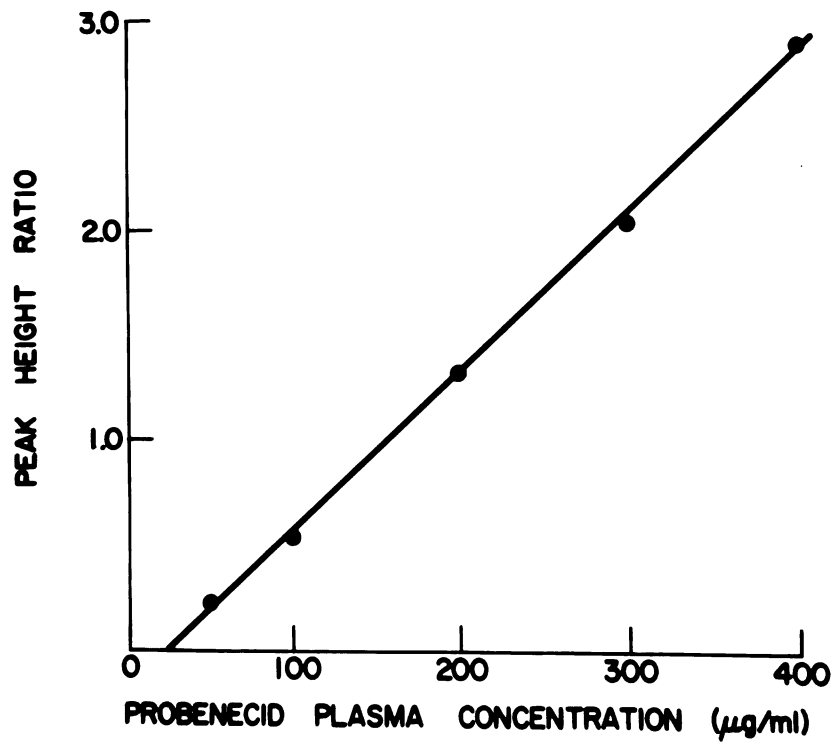


Figure 2-3. Standard curve for probenecid extracted from rat plasma.

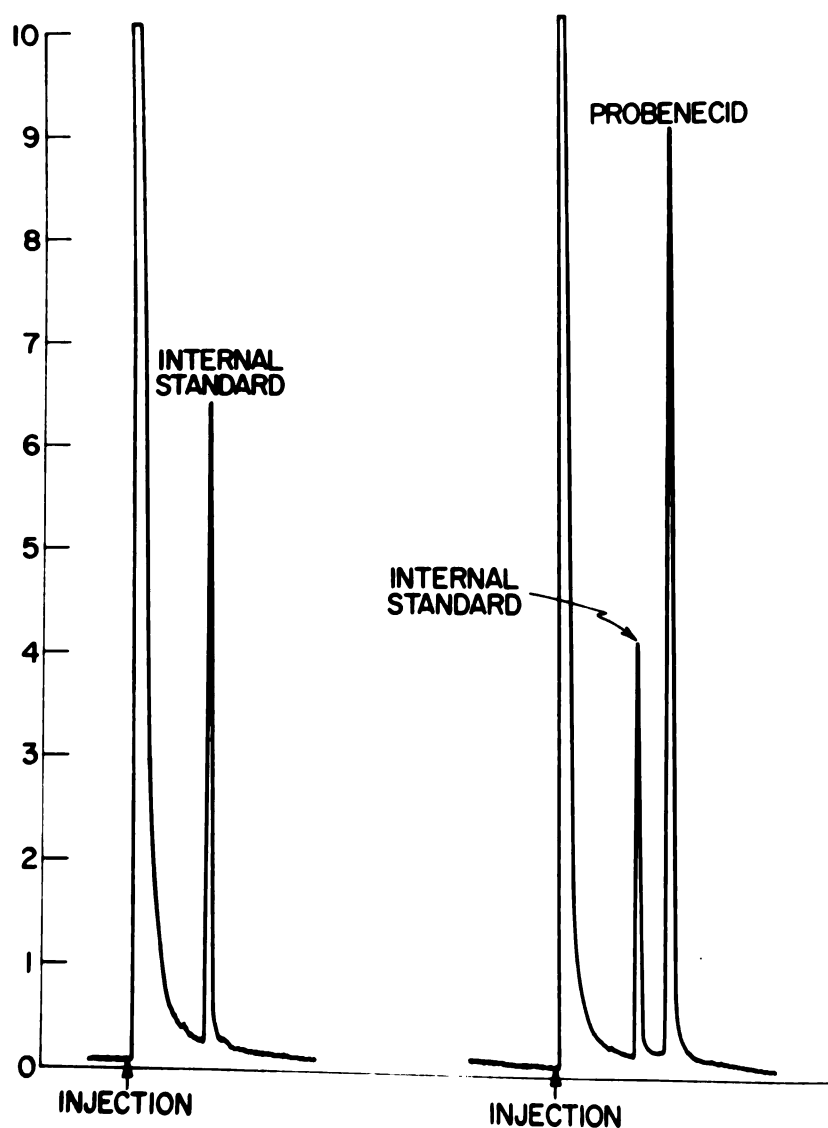


Figure 2-4. Gas-liquid chromatography recording for extractions of probenecid from rat plasma. The tracing on the left is a typical control plasma sample with internal standard added. The tracing on the right is a typical plasma sample obtained from a probenecid treated rat. The instrument conditions were as follows: Column temperature - 230°, Injector temperature - 275°, Detector temperature, 275°, Nitrogen flow rate - 40 ml/min, Hydrogen flow rate - 50 ml/min, Oxygen flow rate - 60 ml/min.

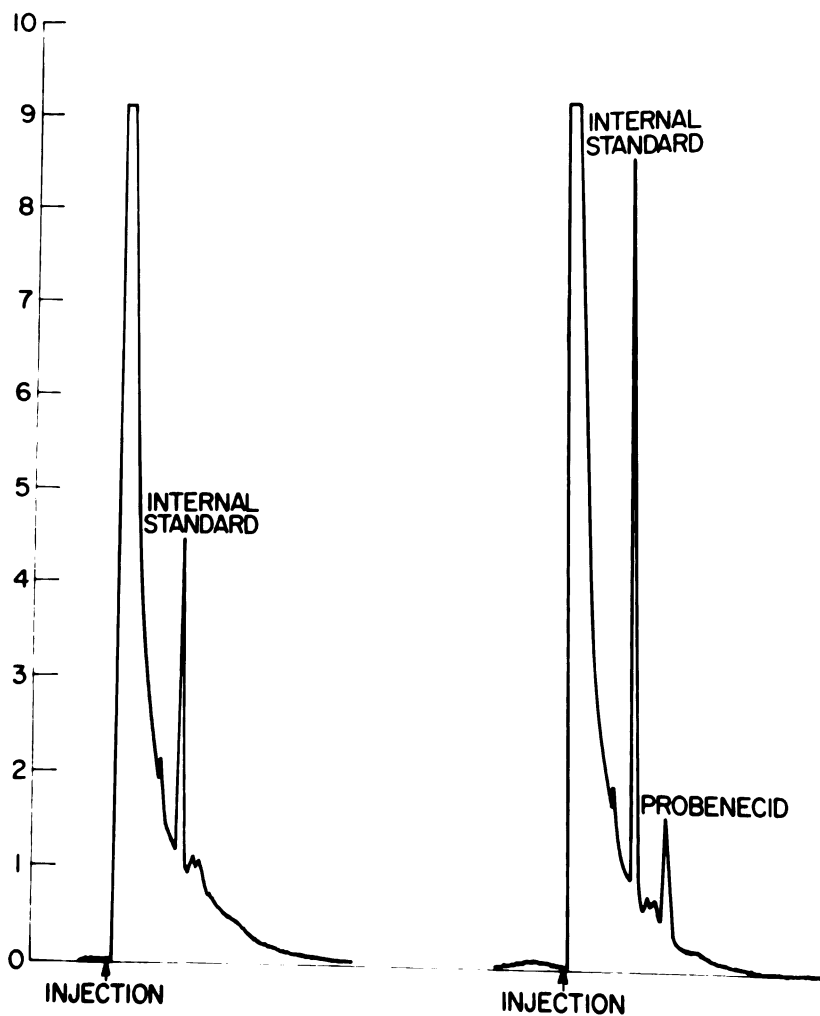


Figure 2-5. Gas-liquid chromatography recording for extractions of probenecid from rat brain. The tracing on the left is a typical control brain sample with internal standard added. The tracing on the right is a typical brain sample obtained from a probenecid treated rat. The instrument conditions were the same as in Figure 2-4.

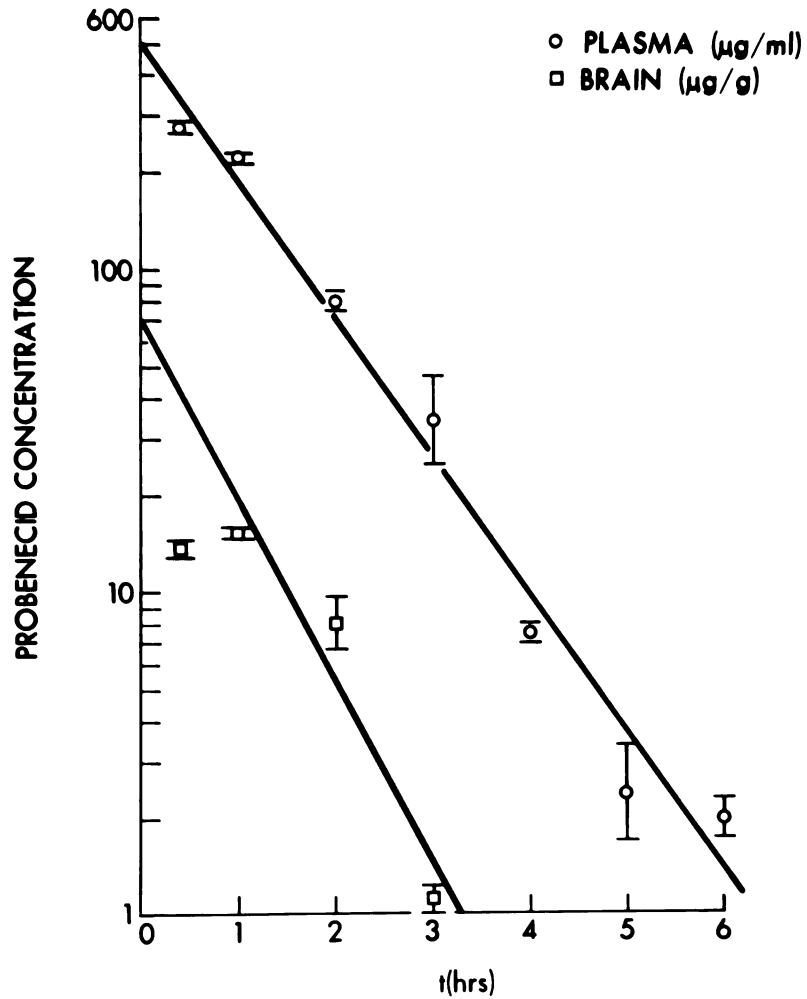


Figure 2-6. Semi-logarithmic plots of rat plasma and brain probenecid levels after a 100 mg/kg intraperitoneal dose of probenecid.

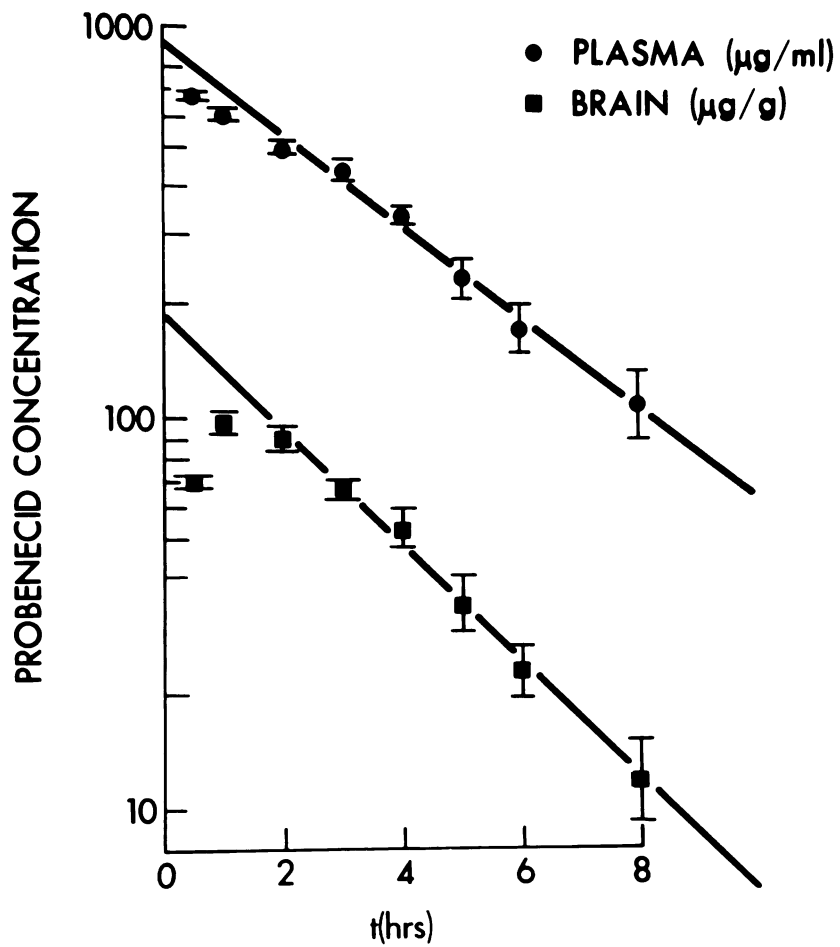


Figure 2-7. Semi-logarithmic plots of rat plasma and brain probenecid levels after a 300 mg/kg intraperitoneal dose of probenecid.

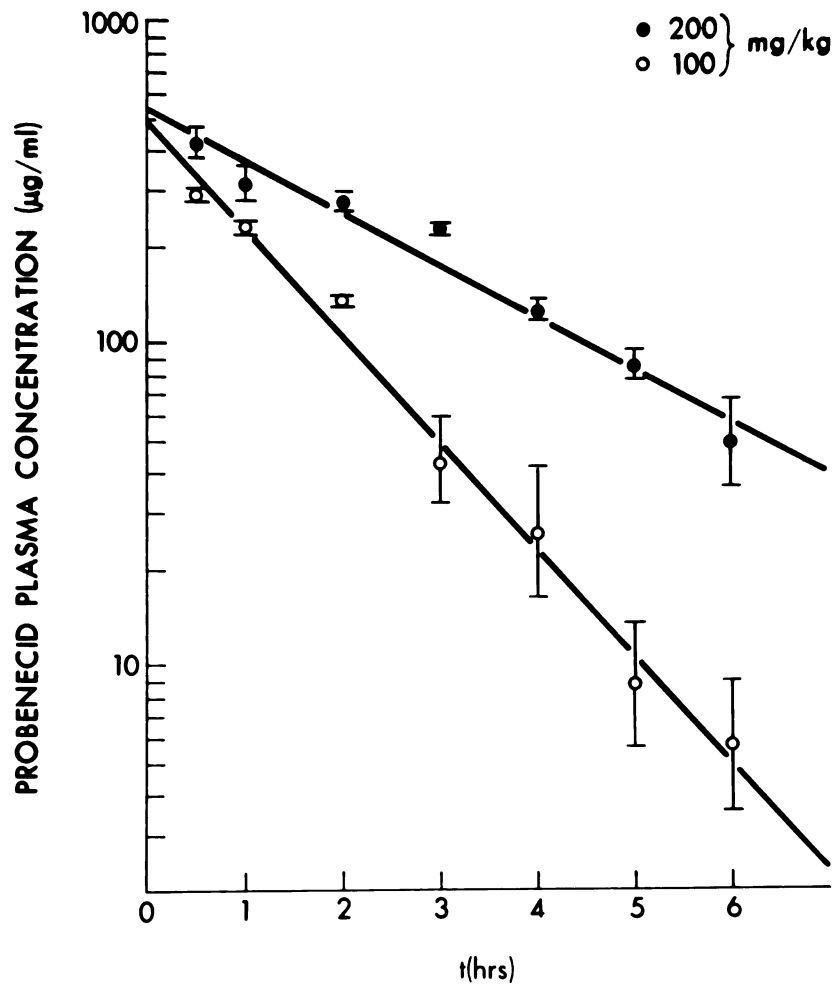


Figure 2-8. Semi-logarithmic plots of rat plasma probenecid concentrations after 100 and 200 mg/kg intraperitoneal doses of probenecid. Data from previous experiments by Tozer (29).

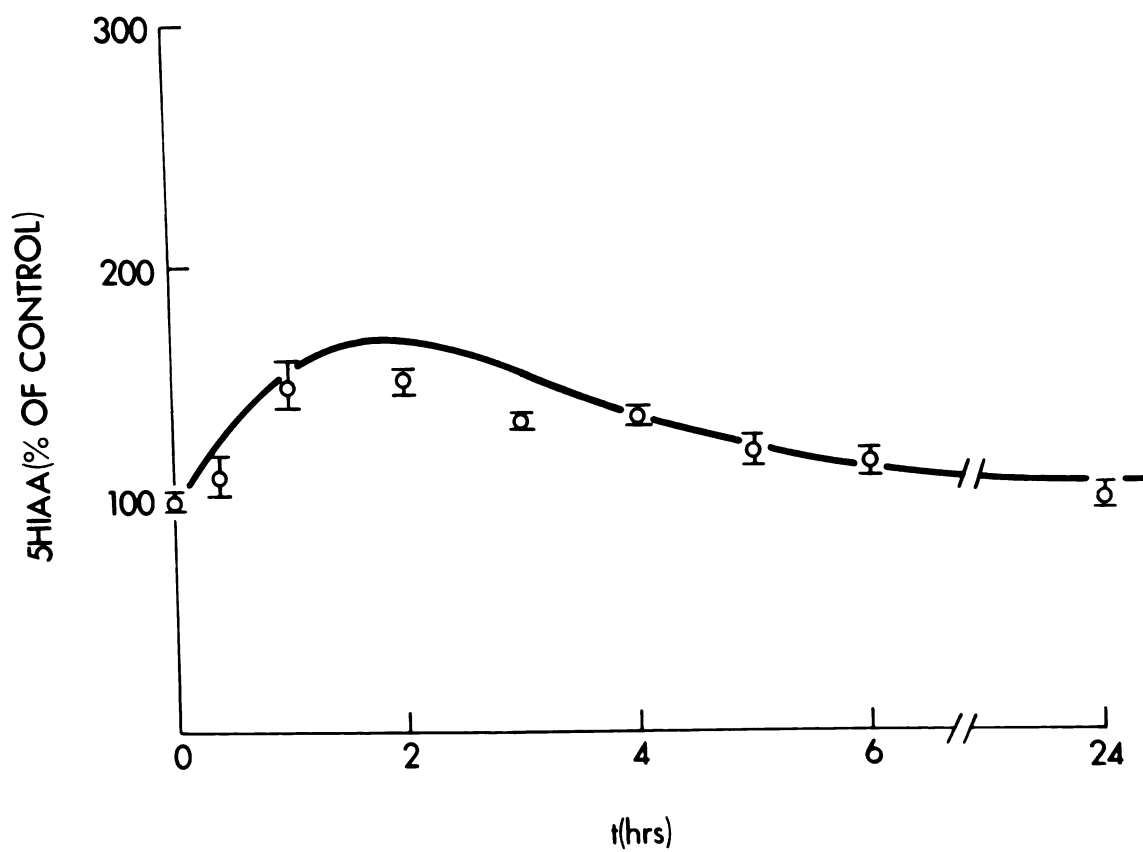


Figure 2-9. Rat brain 5HIAA levels, expressed as percent of control, following a 100 mg/kg intraperitoneal dose of probenecid. The line drawn through the points is the curve of best fit generated by an analog computer.

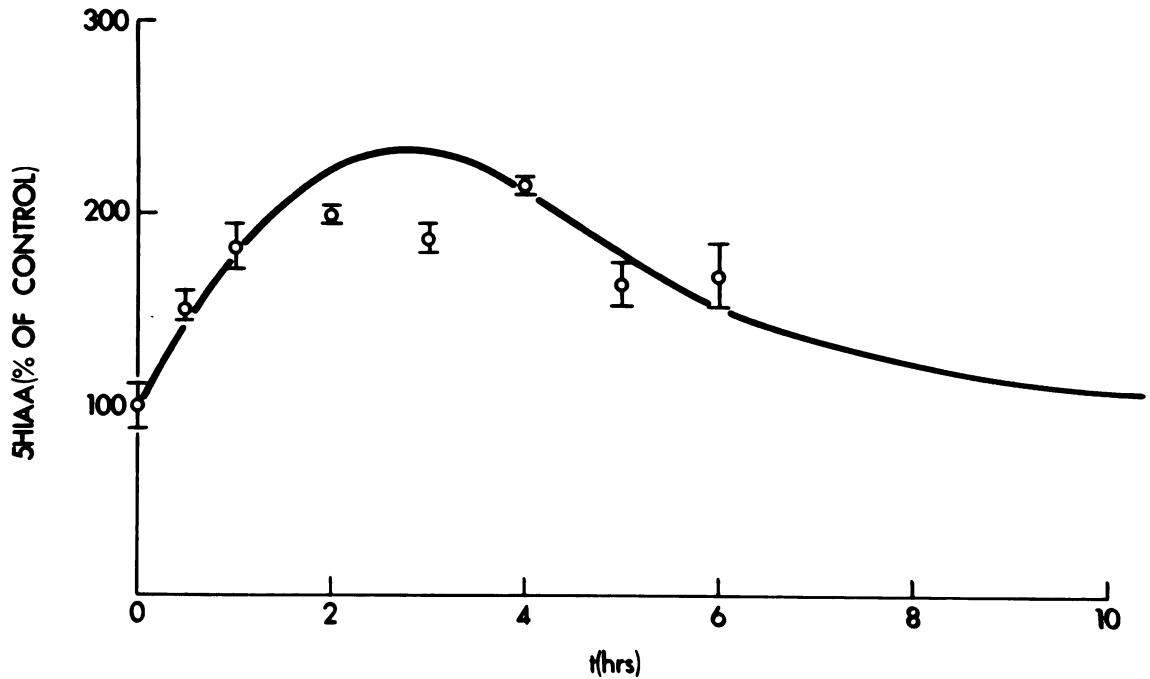


Figure 2-10. Rat brain 5HIAA levels, expressed as percent of control, following a 100 mg/kg intraperitoneal dose of probenecid. The line drawn through the points is the curve of best fit generated by an analog computer. The figure was prepared from Tozer's data (29).



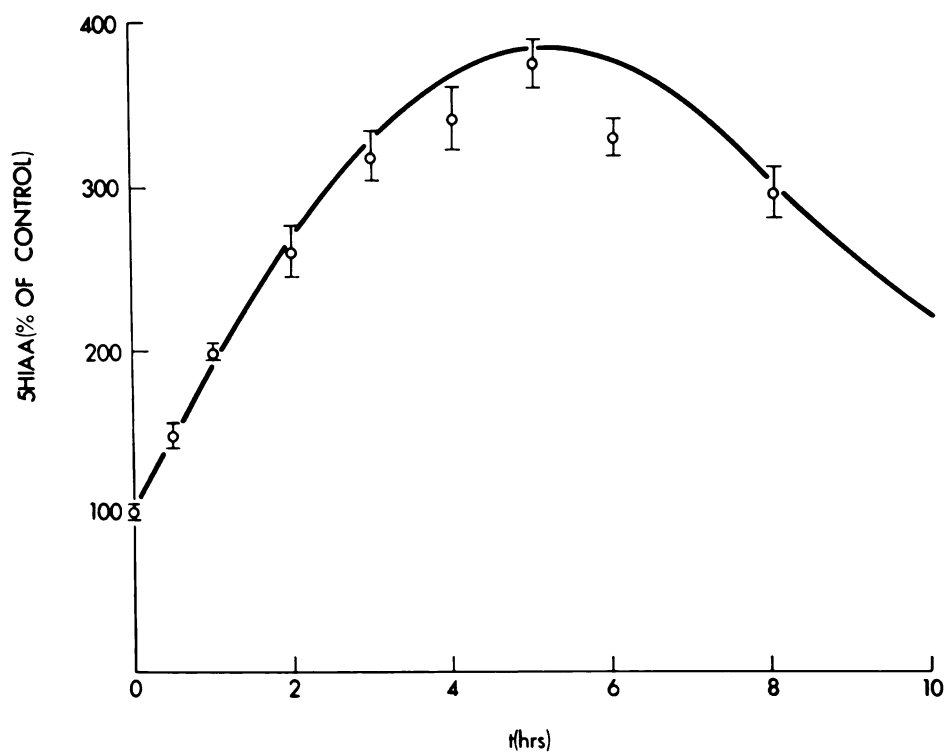


Figure 2-11. Rat brain 5HIAA levels, expressed as percent of control, following a 300 mg/kg intraperitoneal dose of probenecid. The line drawn through the points is the curve of best fit generated by an analog computer.

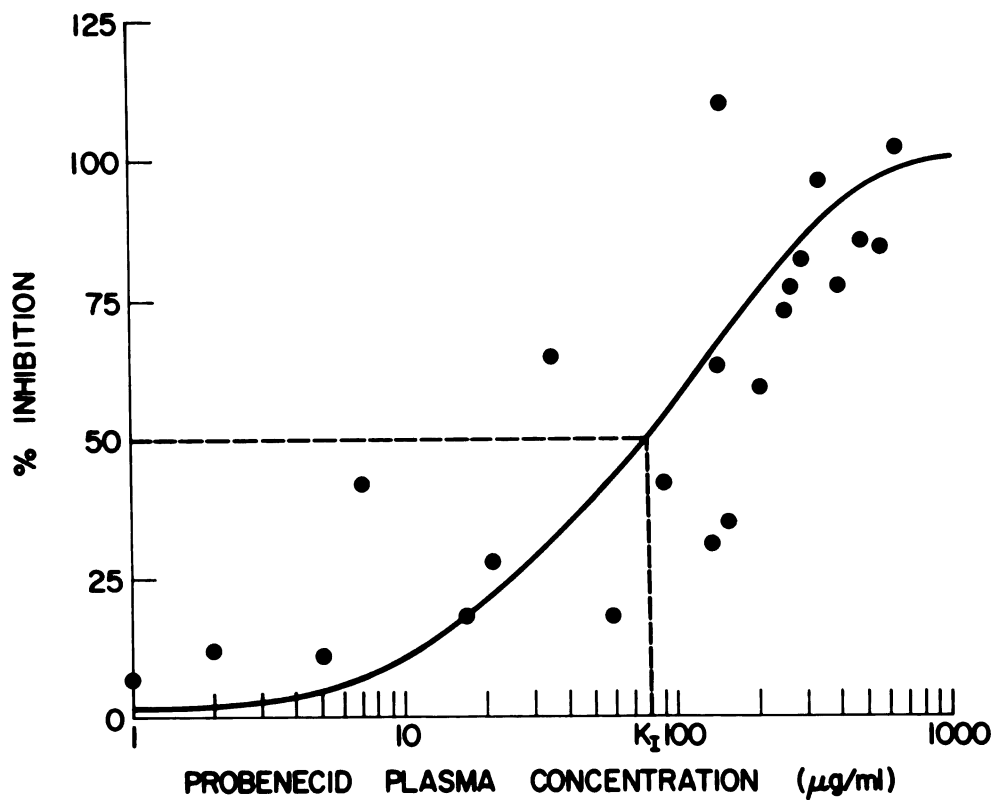


Figure 2-12. Calculated percent inhibition values versus the logarithm of the corresponding probeneqid plasma concentrations.

## CHAPTER III

### TRANSPORT OF SALICYLIC ACID FROM THE BRAIN

#### Section 1: Introduction

As previously discussed in the introductory chapter the objectives of the present investigation could best be met by studying the transport of both endogenous and exogenous acids. The previous chapter dealt with the endogenous acid 5HIAA. This chapter will report on the results of a study of the acid transport system using an exogenous compound, salicylic acid.

By an exogenous acid is meant a compound which is not normally found in the central nervous system of a rat and therefore must enter the central nervous system from the general circulation. To study the acid transport system from brain to blood utilizing an exogenous acid is important because most drugs are exogenous compounds. The existence of transport systems for the elimination of organic acids from the brain and cerebrospinal fluid has been documented in Chapter I. It was Steinwall (13), however, who first made the interesting proposal that a transport system for organic acids in the brain could conceivably function as a component of the blood-brain barrier by pumping out exogenous acids as rapidly as they diffuse into the central nervous system from the blood. His studies supporting his theories have already been summarized in Chapter I.

Confirmation of an acid transport system in the brain

requires knowledge of a number of factors governing the distribution and disposition of exogenous acids in the brain, for example, binding to blood proteins and tissue components, metabolism of the drug, diffusion in and out of the brain, and bulk flow of the cerebrospinal fluid. This chapter is concerned with presenting a model to detect the presence of facilitated transport or other saturable processes which would influence the disposition of an acid in the brain. The model was experimentally tested utilizing salicylic acid as an exogenous acid. Salicylic acid was chosen because it had been previously reported by Mayer, et al. (5) that salicylic acid in the brain failed to reach an equilibrium with the unbound drug in the plasma, although the plasma level of the drug was maintained at a steady state.

## Section 2: Theoretical

Consider the simplest model for the distribution of drugs into tissues, the case in which a drug enters and leaves a tissue only by passive diffusion. For such a system the change in the amount of drug in the tissue with time,  $\frac{dT}{dt}$ , may be expressed by an equation based on Fick's first law of diffusion and the assumption that only unbound drug is diffusible:

$$\frac{dT}{dt} = k (C_1 - C_2) \quad (18)$$

where  $C_1$  is the concentration of drug in the plasma free from protein binding,  $C_2$  is the unbound concentration of drug in the tissue, and  $k$  represents a hybrid constant (units of

clearance) for passage of the drug between plasma and tissue. The rate of entry of the drug into the tissue is  $kC_1$ , while  $kC_2$  is the rate of exit of the drug from the tissue. The integral of the rate of entry with time is the amount entering the tissue,  $\int_0^{\infty} kC_1 dt$ , while the integral of the rate of exit with time equals the amount leaving the tissue,  $\int_0^{\infty} kC_2 dt$ . The total amount that enters the tissue must equal the total amount that leaves the tissue; therefore,

$$\int_0^{\infty} C_1 dt = \int_0^{\infty} C_2 dt \quad (19)$$

Passive diffusion requires that the area under the unbound plasma concentration-time curve be equal to the area under the unbound tissue concentration-time curve.

In an experiment in which steady-state plasma and tissue levels are attained, that is  $\frac{dT}{dt} = 0$ , then from Equation 18

$$C_1^{SS} = C_2^{SS} \quad (20)$$

where  $C_1^{SS}$  is the unbound plasma concentration at steady state, and  $C_2^{SS}$  is the unbound tissue concentration at steady state. The same relationship would be applicable for an experiment in which a single dose is administered. At the point in time,  $t$ -max, when the rates into and out of the tissue are equal, the unbound tissue level is maximal,  $C_2^{\max}$ , and equal to the unbound plasma concentration,  $C_1^{t-\max}$ ,

$$C_1^{t-\max} = C_2^{\max} \quad (21)$$

Plasma and Tissue Binding: Unbound concentrations of a drug are not readily determined, particularly within a tissue. Usually, the total plasma concentration,  $C_p$ , and the total tissue concentration,  $C_T$ , are measured. The total plasma and tissue concentrations are complex functions of their respective unbound concentrations. The functions depend on the affinity of a drug for the plasma proteins and tissue components and on the total number of binding sites. The unbound concentration of the drug in the plasma is a fraction,  $\alpha_1$ , of the total plasma concentration,

$$C_1 = \alpha_1 C_p \quad (22)$$

The fraction unbound will vary with the total plasma concentration and thus with the dose. Consequently, the relationship between the area under the unbound concentration-time curve to the area under the total concentration-time curve becomes a function of the dose. This ratio can be thought of as the ratio of the mean value of  $C_1$  with time,  $\bar{C}_1$ , to the mean value of  $C_p$  with time,  $\bar{C}_p$ , that is, the ratio of the time average values,

$$\frac{\int_0^{\infty} C_1 dt}{\int_0^{\infty} C_p dt} = \frac{\int_0^{\infty} C_1 dt / \int_0^{\infty} dt}{\int_0^{\infty} C_p dt / \int_0^{\infty} dt} = \frac{\bar{C}_1}{\bar{C}_p} \quad (23)$$

Similarly for the tissue,

$$C_2 = \alpha_2 C_T \quad (24)$$

where  $\alpha_2$  is the fraction of drug in the tissue which is not bound to tissue components. Therefore,

$$\frac{\int_0^{\infty} C_2 dt}{\int_0^{\infty} C_T dt} = \frac{\bar{C}_2}{\bar{C}_T} \quad (25)$$

As the areas under the unbound plasma concentration-time curve and the unbound tissue concentration-time curve must be equal (Equation 19),  $\bar{C}_1$  equals  $\bar{C}_2$ . Dividing Equation 23 by Equation 25 yields

$$R = \frac{\int_0^{\infty} C_T dt}{\int_0^{\infty} C_P dt} = \frac{\bar{C}_T}{\bar{C}_P} \quad (26)$$

The ratio,  $R$ , which shall be referred to as the area distribution ratio, is a measure of the concentration of drug in the tissue with time relative to that in the plasma with time. For both plasma and tissue the fraction of the drug unbound normally increases with concentration; as the dose is increased, therefore,  $\frac{\bar{C}_1}{\bar{C}_P}$  and  $\frac{\bar{C}_2}{\bar{C}_T}$  will increase. An increase or decrease of  $R$  with increasing dose will depend on whether the plasma protein binding or tissue binding is the more readily saturable. The former will result in an increase in  $R$ , the latter in a decrease.

In steady-state experiments the fractions unbound in plasma,  $\alpha_1^{ss}$ , and in tissue,  $\alpha_2^{ss}$ , are

$$\alpha_1^{ss} = \frac{C_1^{ss}}{C_P^{ss}} \quad (27)$$

$$\alpha_2^{ss} = \frac{C_2^{ss}}{C_T^{ss}} \quad (28)$$

The total plasma and tissue concentrations at steady state are represented by  $C_P^{SS}$  and  $C_T^{SS}$ , respectively. As given in Equation 20, the steady state unbound concentrations in plasma and tissue are equal; therefore, dividing Equation 27 by Equation 28 yields a steady state distribution ratio,  $R^{SS}$ ,

$$R^{SS} = \frac{C_T^{SS}}{C_P^{SS}} = \frac{\alpha_1^{SS}}{\alpha_2^{SS}} \quad (29)$$

Similarly in an experiment in which a single dose is given, there is a time,  $t\text{-max}$ , when the unbound tissue concentration equals the unbound plasma concentration as given in Equation 21. The total concentration in the tissue,  $C_T^{\max}$ , will be at a maximum at the same point in time when  $C_2^{\max}$  is achieved assuming tissue binding is instantaneous. A  $t\text{-max}$  distribution ratio,  $R^{\max}$ , may then be defined as follows:

$$R^{\max} = \frac{C_T^{\max}}{C_P^{\max}} = \frac{\alpha_1^{\max}}{\alpha_2^{\max}} \quad (30)$$

The plasma concentration at the same time point when the tissue is at the maximum concentration is defined as  $C_P^{t\text{-max}}$ . The values of  $R^{SS}$  and  $R^{\max}$  will vary with dose in a similar fashion to  $R$  due to the decreased binding at higher concentrations.

Saturable Transport Systems: The presence of transport, metabolic, or excretory mechanisms will also give rise to a change in  $R$ ,  $R^{SS}$ , and  $R^{\max}$  with dose as determined by Equations 26, 29, and 30. As an example consider the case in which the rate of entry into a tissue may be kinetically



expressed as a combination of passive diffusion and a saturable transport. For such a case,

$$\text{Rate in} = kC_1 + \frac{aC_1}{b + C_1} \quad (31)$$

The maximum rate of transport is represented by  $a$ ;  $b$  is the dissociation constant for the "drug-carrier" complex, and  $k$  is as defined in Equation 18. The amount that enters the tissue is obtained by integration of Equation 31,

$$\text{Amount entering tissue} = k \int_0^{\infty} C_1 dt + a \int_0^{\infty} \frac{C_1}{b + C_1} dt \quad (32)$$

Assuming that a drug leaves the tissue only by passive diffusion, the total amount which leaves the tissue is  $k \int_0^{\infty} C_2 dt$  as shown in the derivation of Equation 19. Furthermore, if the assumption is made that no protein binding occurs in the plasma or tissue, substituting  $C_P$  for  $C_1$  and  $C_T$  for  $C_2$  leads to the following:

$$k \int_0^{\infty} C_T dt = k \int_0^{\infty} C_P dt + a \int_0^{\infty} \frac{C_P}{b + C_P} dt \quad (33)$$

that is, the total amount which leaves the tissue must equal that which enters the tissue. The area distribution ratio as expressed in Equation 26 becomes

$$R = 1 + \frac{\frac{a}{k} \int_0^{\infty} \frac{C_P}{b + C_P} dt}{\int_0^{\infty} C_P dt} \quad (34)$$

The transport into the tissue gives rise to values of  $R$  greater than 1; however, as the dose is increased to the point

that  $C_p$  exceeds  $b$  for prolonged periods the value of  $R$  will decrease toward a value of unity.

Conversely, transport out of the tissue with passive diffusion in and out of the tissue and no plasma or tissue binding, will result in the following:

$$\text{rate in} = kC_p \quad (35)$$

$$\text{rate out} = kC_T + \frac{a' C_T}{b' + C_T} \quad (36)$$

for which  $a'$  is the maximum rate of transport out and  $b'$  is the dissociation constant for the drug-carrier complex. Since the total amount entering the tissue equals the total amount leaving the tissue

$$k \int_0^{\infty} C_p dt = k \int_0^{\infty} C_T dt + a' \int_0^{\infty} \frac{C_T}{b' + C_T} dt \quad (37)$$

the area distribution ratio then becomes

$$R = 1 - \frac{\frac{a'}{k} \int_0^{\infty} \frac{C_T}{b' + C_T} dt}{\int_0^{\infty} C_p dt} \quad (38)$$

In this case  $R$  is less than unity and an increase in dose gives rise to an increase in its value toward unity. The same argument holds for saturable metabolism or excretory mechanisms in the tissue.

For the steady state condition, if a transport into the tissue is present as expressed in Equation 31 and only passive diffusion accounts for the exit of the drug, then assuming no binding effects the rate out of the tissue,  $kC_T$ ,

must equal  $kC_p + \frac{aC_p}{b + C_p}$ , the rate into the tissue. A steady state distribution ratio will then be defined by the following:

$$R^{ss} = 1 + \frac{a}{k(b + C_p^{ss})} \quad (39)$$

For transport out of the tissue:

$$R^{ss} = 1 - \frac{\frac{a'}{k} C_T^{ss}}{C_p^{ss} (b' + C_T^{ss})} \quad (40)$$

Following a bolus dose, the t-max distribution ratios will be identical to Equations 39 and 40;  $C_T^{\max}$  and  $C_p^{t-\max}$  replace  $C_T^{ss}$  and  $C_p^{ss}$ , respectively, in the equations above.

A change in a distribution ratio with dose is indicative of the existence of nonlinear disposition of a drug in a tissue. As previously discussed the direction of change in the distribution ratio with dose gives an indication as to which nonlinear process might exist. In reality, however, combinations of saturable processes are likely to be present. Figure 3-1 schematically shows the mechanisms which would result in a dose-dependent distribution ratio. For combinations of saturable processes the net change in the distribution ratio is a result of the dominant process if the effects are opposite. If the effects reinforce each other, the change is exaggerated. An increase or decrease in a distribution ratio with dose could thus help discern which saturable process is involved; for example:

IF A DISTRIBUTION RATIO DECREASES WITH DOSE,

1. a unidirectional transport into the tissue may exist. Such a transport is described by process a in Figure 3-1. As the dose increases, the transport system approaches saturation, resulting in tissue concentrations of the drug which are proportionately lower at the higher plasma concentrations.
2. tissue binding of the drug may be occurring, process b. The possibility in this case is one of saturation of binding sites within the tissue as the dose increases. The apparent effect would be that the tissue loses the ability to accumulate the drug.
3. metabolism of the drug in the tissue may be increasing, process c. This is an unlikely possibility unless the drug activates its own metabolism or the experiment involves chronic dosing with a drug which induces its own metabolizing enzymes.

IF A DISTRIBUTION RATIO INCREASES WITH DOSE,

1. the degree of plasma protein binding may not be constant as the dose is increased, process e in Figure 3-1. This is to be expected, since the fraction of drug unbound normally increases with concentration.
2. a metabolic or an excretory system capable of being saturated may exist in the tissue, processes c and d, respectively. The administration of increasing

doses will result in a lower rate of elimination relative to the amount in the tissue. The net result would be an increase in tissue levels larger than the corresponding increase in plasma levels.

3. elimination from the tissue may involve a saturable transport system, process f.

Correction for Plasma Protein Binding: An increase in a distribution ratio with dose due to the saturation of plasma protein binding can be readily ascertained. Assuming that the entry of a drug into a tissue depends upon the unbound drug in plasma, the ratio of the area under the tissue concentration-time curve to the area under the unbound plasma concentration-time curve would be independent of plasma protein binding. This ratio may be determined by dividing Equation 26 by Equation 23,

$$R_{\text{COR}} = \frac{\int_0^{\infty} C_T dt}{\int_0^{\infty} C_1 dt} \quad (41)$$

The ratio,  $R_{\text{COR}}$ , will be referred to as the area distribution ratio corrected for plasma protein binding.

A steady state distribution ratio corrected for plasma protein binding,  $R_{\text{COR}}^{\text{SS}}$ , may be determined from steady state tissue and unbound plasma concentrations

$$R_{\text{COR}}^{\text{SS}} = \frac{C_T^{\text{SS}}}{C_1^{\text{SS}}} \quad (42)$$

Similarly, following a single dose, the t-max distribution ratio corrected for plasma protein binding is

$$R_{\text{cor}}^{\text{max}} = \frac{C_{\text{T}}^{\text{max}}}{C_{\text{I}}^{\text{t-max}}} \quad (43)$$

The values of  $R_{\text{cor}}$ ,  $R_{\text{cor}}^{\text{ss}}$ , and  $R_{\text{cor}}^{\text{max}}$  should be unity unless tissue binding or other saturable processes occur in the tissue. If the distribution ratios corrected for protein binding do not change over the dosage range tested, saturation of plasma protein binding is the mechanism by which  $R$ ,  $R^{\text{ss}}$ , and  $R^{\text{max}}$  vary with dose. Any change in the corrected distribution ratios indicates the existence of other saturable processes. The direction of the change gives a further indication of the probable mechanisms.

### Section 3: Experimental

Materials: Fisher Certified Grade Sodium Salicylate was used in this study. Other materials used were listed in Chapter II, Section 3, under Materials.

Animals: Male Sprague-Dawley rats weighing 190-210 g were obtained from Horton Laboratories, Inc., Oakland, California, and used throughout this study.

Apparatus: Aminco-Bowman spectrophotofluorometer model 8210, Dianorm<sup>®</sup> equilibrium dialysis system supplied by Innovativ-Medizin AG., P.O. Box 31, CH-Esslingen, Switzerland. Other equipment used is listed in Chapter II, Section 3, under Apparatus.

Experimental Design: Two major studies were carried out. In one, the rats received a dose of sodium salicylate corresponding to 25 mg/kg; in the other, the dose was 400

mg/kg. Several groups of animals with five rats per group were randomly selected for each study. Except for the control group, each rat received an intraperitoneal injection of 1 ml of a sodium salicylate solution. After treatment the animals were sacrificed at different times by decapitation. Upon decapitation the blood from each rat was collected in a 50 ml beaker containing 200  $\mu$ l of 0.05 M solution of (ethylenedinitrilo)tetraacetic acid disodium salt. After centrifugation of the blood, 1 ml of plasma was transferred to a centrifuge tube. The brain from each rat was removed after decapitation and quickly frozen in dry ice after blotting with a tissue to remove excess surface blood. Brain and plasma samples were stored frozen until the time of analysis.

Assay Procedures: Plasma samples were assayed using the procedure of Rowland and Riegelman (30). Standard curves were prepared by extracting control plasma samples containing known amounts of salicylic acid. Figure 3-2 is an example of a standard curve prepared from control plasma.

To assay the brain samples for salicylic acid, each brain was homogenized in a Tenbroeck tissue grinder using two volumes of distilled water for every gram of brain. Three ml of homogenate were transferred into a 20 ml culture tube containing approximately 2 g of sodium chloride and 0.3 ml of 6 N HCl. After mixing the samples, 5 ml of a solution of equal volumes of ether and n-heptane were added to the samples, and the samples were gently shaken on a mechanical shaker for 30 minutes. After centrifugation to separate

the phases, an aliquot of the organic phase was extracted with 2 ml of a 0.5 M phosphate buffer pH 7. The phosphate buffer extracts were read on the spectrophotofluorometer at the wavelengths for maximum activation and fluorescence as determined using a standard sample of sodium salicylate in phosphate buffer. Using the extraction procedure as described, known amounts of salicylic acid were added to homogenates of control brains to prepare the standard curves. Figure 3-3 is an example of such a standard curve. Standard curves were always prepared on the same day an assay of blood or brain samples was to be carried out.

The value obtained for the amount of salicylic acid per gram of brain tissue had to be corrected for the contribution of drug from the residual blood which remains in the brain after decapitation. The amount of residual blood per gram of rat brain has been reported to be 11  $\mu$ l (31). Using this value for the residual blood in brain and calculating the concentration of salicylic acid in the blood from the concentration in plasma (refer to Appendix B), it was possible to determine the amount of salicylic acid that had to be subtracted from the amount assayed in the brain.

Protein Binding Study: The degree of plasma protein binding for salicylic acid was determined using the Dianorm<sup>®</sup> equilibrium dialysis system. The apparatus consists of 20 Teflon<sup>®</sup> cells, each of which is divided into two compartments or half-cells with a 1 ml volume by a section of Visking<sup>®</sup> tubing with a thickness of 0.025 mm. The cells are mounted



on a rotor such that agitation is accomplished by rotation of the cells. The entire apparatus is water tight so that it may be immersed in a constant temperature water bath.

In the present study 1 ml of a solution of sodium salicylate in Krebs-Ringer bicarbonate buffer was introduced with a tuberculin syringe into one half-cell, and 1 ml of fresh rat plasma was simultaneously injected into the other half-cell. Since the apparatus has 20 cells, it was possible to dialyze different concentrations of salicylic acid at one time. Preliminary experimentation showed equilibrium to be reached within 1-2 hours; therefore, the dialysis was carried out for 3 hours at 37°. After equilibration, the solutions in the buffer and plasma half-cells were analyzed using the plasma assay previously mentioned. The concentration of drug in the buffer half-cell was taken to represent the concentration of the free ligand on both sides of the membrane. The total concentration of the bound and free ligand was obtained from the analysis of the plasma half-cell. The fraction of salicylate unbound was thus calculated by dividing the concentration in the buffer half-cell by the concentration in the plasma half-cell.

#### Section 4: Results and Discussion

The salicylate concentrations assayed in plasma and brain are summarized in Table IX. The samples were analyzed separately; the values reported are the arithmetic means of five separate plasma or brain samples.

TABLE IX  
SALICYLIC ACID DISPOSITION IN THE RAT BRAIN  
AND PLASMA

Hours after Treatment	Total Plasma Concentration* ( $\mu\text{g/ml}$ )	Assayed Brain Concentration* ( $\mu\text{g/g}$ )
<u>25 mg/kg Dose</u>		
0.5	105.8 $\pm$ 1.9	3.98 $\pm$ .45
1.0	96.5 $\pm$ 2.3	4.16 $\pm$ .30
5.0	65.2 $\pm$ 4.3	2.89 $\pm$ .16
10.0	15.2 $\pm$ 2.8	0.60 $\pm$ .08
15.0	8.5 $\pm$ 1.2	0.26 $\pm$ .03
20.0	4.2 $\pm$ 1.2	0.12 $\pm$ .04
<u>400 mg/kg Dose</u>		
1.0	561.2 $\pm$ 41.7	119.7 $\pm$ 15.4
5.0	380.4 $\pm$ 14.4	71.9 $\pm$ 3.0
10.0	357.6 $\pm$ 22.7	62.4 $\pm$ 4.5
20.0	187.7 $\pm$ 14.7	21.3 $\pm$ 2.5
30.0	153.0 $\pm$ 5.1	12.1 $\pm$ 1.0
40.0	62.3 $\pm$ 12.8	3.4 $\pm$ 0.8
50.0	26.2 $\pm$ 7.2	1.2 $\pm$ 0.4

\*The mean of five animals and standard error.

The results of the plasma protein binding study are depicted in Figure 3-4. Using this graph the values for total salicylate in plasma,  $C_p$ , in Table IX, were converted to the concentrations of unbound salicylic acid,  $C_1$ . The brain concentrations reported in Table IX were corrected for the salicylic acid contributed by the residual blood as discussed above. The corrected tissue concentrations,  $C_T$ , together with the unbound concentrations of salicylic acid in plasma are plotted in Figure 3-5.

The disposition of salicylic acid in rats is dose-dependent, as evidenced by the difference in the apparent half lives of elimination for the 25 and 400 mg/kg doses. A comparison of the half lives calculated from the slopes of the plasma curves in Figure 3-5 within the first 20-30 hours accentuates the dose-dependency. The half life of salicylic acid in the plasma after a 25 mg/kg dose was 2.8 hours, while a half life of 11 hours resulted from a 400 mg/kg dose. Dose-dependent elimination of salicylic acid in man has been previously reported by Levy, et al.(32). These authors pointed out that monoexponential fits of plasma data are incorrect and that nonlinear kinetics best describes salicylic acid disposition; however, these conclusions are based on studies in individuals. For such studies, nonlinear kinetic parameters can be obtained by curve fitting the data from each individual. In the present investigation a population study is involved; therefore, calculations of nonlinear parameters are not as valid as when an individual is the test subject.

Dose-dependency in the time course of the unbound plasma concentration will give rise to disproportionately larger areas under the  $C_1$ -time curve; since the amount entering a tissue must equal the amount leaving a tissue, the ratio of the areas under the  $C_T$ -time curve to the area under the  $C_1$ -time curve should not change. That is, the distribution ratio is independent of the time course of a drug in the body; saturable processes must be present to account for changes in this ratio with dose.

As presented in Section 2, Theoretical, the calculation of the distribution ratios  $R$  and  $R^{\max}$  after different doses of a drug serves as a test of the model described by Equations 26 and 30. To determine  $R$ , the areas under the cartesian plots of  $C_T$ -time and  $C_p$ -time were estimated using the trapezoidal rule. To determine  $R^{\max}$ ,  $C_T^{\max}$  is approximated by selecting the highest mean value of  $C_T$  achieved. The plasma concentration obtained at the same time as  $C_T^{\max}$  was used for  $C_p^{t-\max}$ . The results are reported in Table X under the heading  $R$  and  $R^{\max}$ . The large increase in  $R$  and  $R^{\max}$  with increasing dose indicates nonlinear disposition of salicylic acid in the brain. The increase in the distribution ratios could be attributed to a decrease in the fraction of salicylic acid bound in the plasma as the plasma concentration increases. To test this possibility, the distribution ratios corrected for plasma protein binding,  $R_{\text{COR}}$  and  $R_{\text{COR}}^{\max}$ , were calculated from the data in Figure 3-5. The corrected distribution ratios calculated for the two doses are listed in Table X.

TABLE X  
EXPERIMENTALLY DETERMINED DISTRIBUTION RATIOS

Dose, mg/kg	R	$R^{\max}$	$R_{\text{COR}}$	$R_{\text{COR}}^{\max}$
25	0.035	0.035	0.180	0.146
400	0.139	0.205	0.302	0.353

Inasmuch as these distribution ratios increase with dose, metabolism, excretion, or transport out of the brain must be involved in the salicylic acid elimination. Transport involvement in the entry of salicylic acid or tissue binding of the drug in the brain would cause a decrease in the distribution ratios if these processes were solely present. As previously discussed, a combination of processes could be involved, but the change in the distribution ratios will be dependent on the dominant mechanisms. For example, entry and exit of salicylic acid in the brain could both be carrier mediated; however, if the transport out were more readily saturated than the transport in, the distribution ratios will be seen to increase with dose.

As further verification of the dose-dependency of the distribution ratios for salicylic acid,  $R^{\max}$  and  $R_{\text{COR}}^{\max}$  were calculated using literature data for salicylic acid distribution in mice (33, 34). These studies included data for brain, unbound blood, and total blood concentration of salicylic

acid at different times following intraperitoneal administration of 50 to 800 mg/kg. The results of these calculations are summarized in Table XI; the results agree with those of the present study; that is, the distribution ratios increase with dose.

TABLE XI  
DISTRIBUTION RATIOS FOR SALICYLIC ACID IN MICE\*

Dose, mg/kg	$R^{\max}$	$R_{\text{cor}}^{\max}$
50	.153	.305
100	.213	.386
200	.278	.487
400	.294	.506
800	.459	.766

\*Calculated from the data of Sturman, et al. (33) and McArthur, et al. (34).

One interpretation of the changes in the values of the distribution ratios could be the existence of a saturable metabolic pathway in the brain as discussed under Theoretical. This explanation is unlikely since Wolff and Austen (35) reported no salicylate metabolites in rat brains; Sturman, et al. (33) reached the same conclusion in their studies with mice. An alternative explanation is the existence of a saturable transport system which functions to rid the brain of unwanted acidic compounds, in this case salicylic acid. As previously

discussed, if the rate of elimination relative to the amount in the tissue becomes lower due to saturation of the transport system, the tissue levels will increase more than the corresponding increase in plasma levels. This would result in a distribution ratio which increases with dose. The hypothesis that a transport system is responsible for the dose-dependency of the distribution ratios presupposes that there are no major physiological changes produced by the drug under study, although it has been reported that salicylic acid is capable of uncoupling oxidative phosphorylation (36). Especially critical is that the cerebral blood flow remain unchanged throughout the course of the study.

The fact that the values for the distribution ratios corrected for plasma protein binding are always less than one also points to a transport system which prevents salicylic acid in the brain from achieving equilibrium with the plasma. Referring to Equations 41 and 43, if there were tissue binding,  $R_{COR}$  and  $R_{max}$  should be greater than one. McArthur, et al. (34) reported that binding does not occur in brain tissue. The values of  $R_{COR}$  and  $R_{COR}^{max}$ , therefore, should be equal to one if there is no metabolism in the tissue, no transport system, nor other means of drug elimination. Cerebrospinal fluid bulk flow could be invoked as responsible for the elimination of acids from the brain, but this process is not saturable and does not explain the dose-dependency of the corrected distribution ratios. Since the metabolism is considered unlikely, the existence of a saturable transport

system remains as the likely mechanism responsible for the change in the distribution ratios. Furthermore, if it were possible to completely saturate a transport system in the brain, the corrected distribution ratios should approach unity. This is observed to occur with the  $R_{COR}^{max}$  values in Table XI.

Thus the presence of an acid transport system which prevents salicylic acid accumulation in the brain is supported by the dose-dependency of the distribution ratios. While the procedure as outlined in this chapter might not be conclusive proof of an acid transport system, it does utilize a technique which is not as disruptive of the central nervous system as brain perfusion studies or other commonly used procedures.



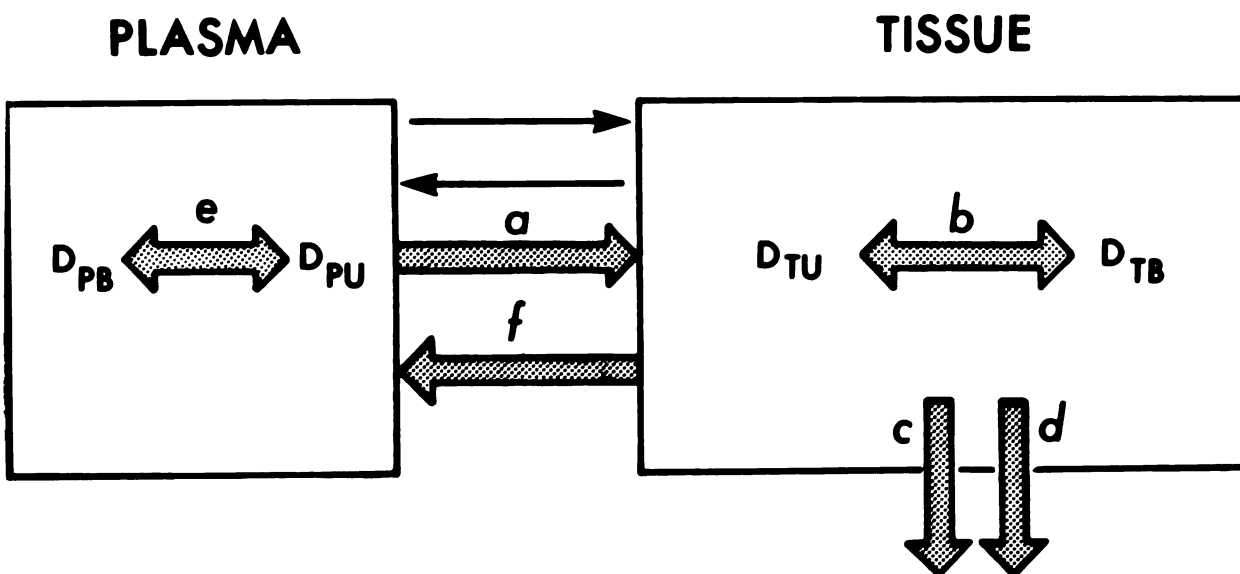


Figure 3-1. Schematic diagram of the processes of disposition of a drug in the brain or any tissue. The thin arrows represent passive diffusion; heavy arrows represent saturable processes. KEY:  $a, f$  - unidirectional transport to and from tissue;  $c$  - metabolism;  $d$  - excretion; and  $b, e$  - binding to tissue components and plasma proteins. Symbols  $D_{PB}$ ,  $D_{PU}$ ,  $D_{TB}$ ,  $D_{TU}$  - Amount of bound and unbound drug in plasma and tissue, respectively.

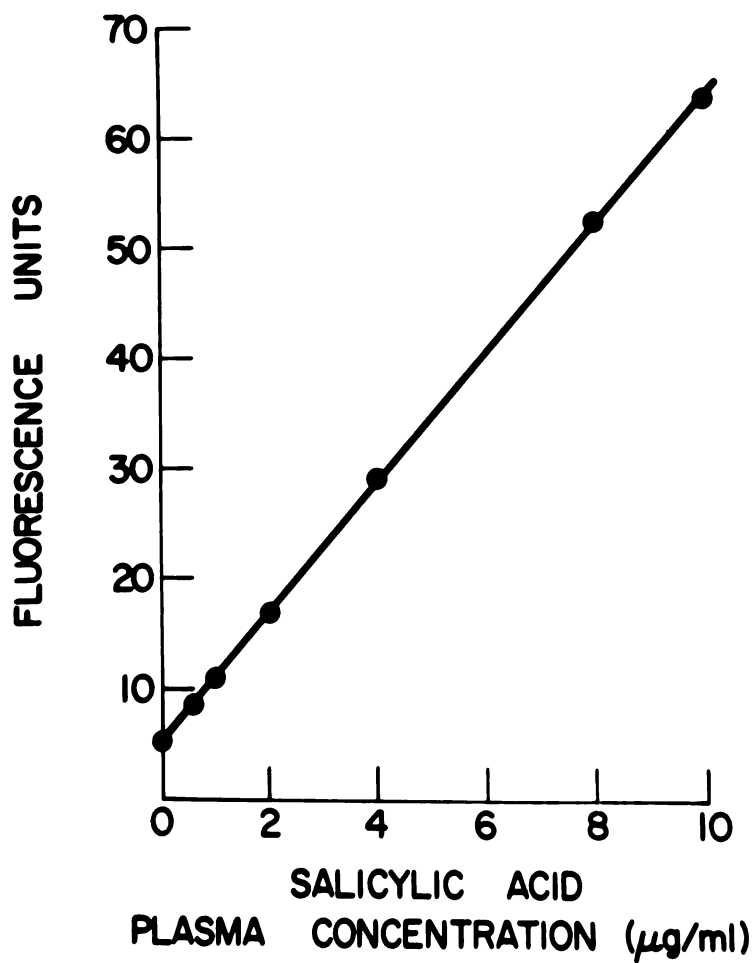


Figure 3-2. Standard curve for salicylic acid extracted from rat plasma. The fluorescence units are arbitrary.

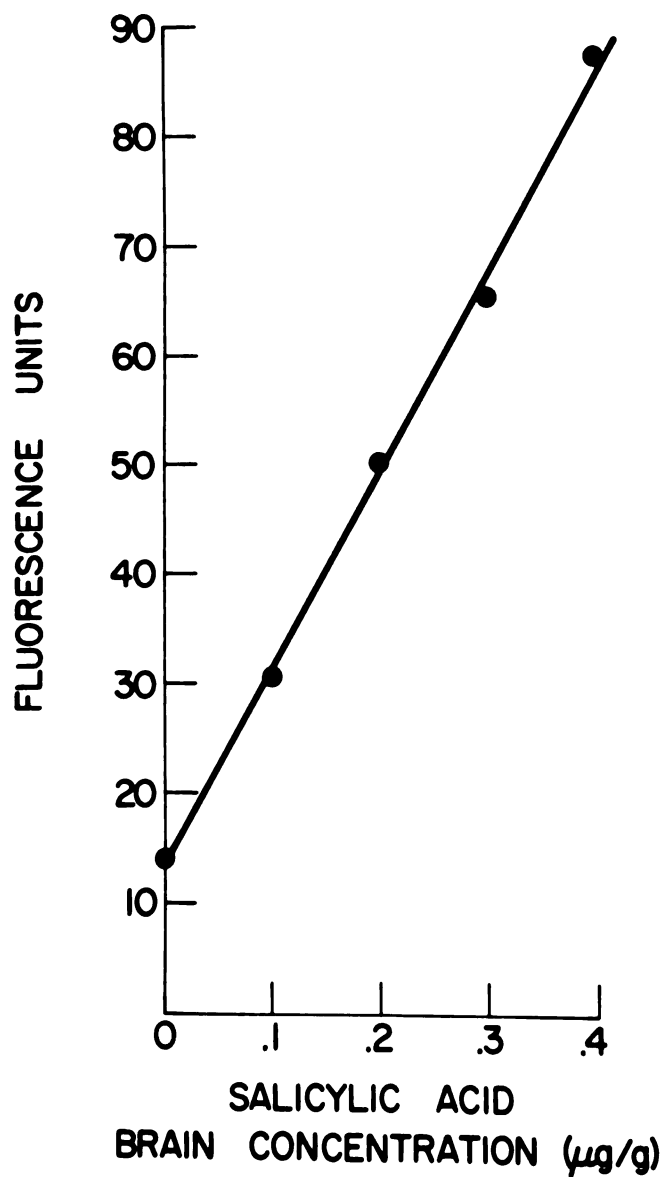


Figure 3-3. Standard curve for salicylic acid extracted from rat brain. The fluorescence units are arbitrary.

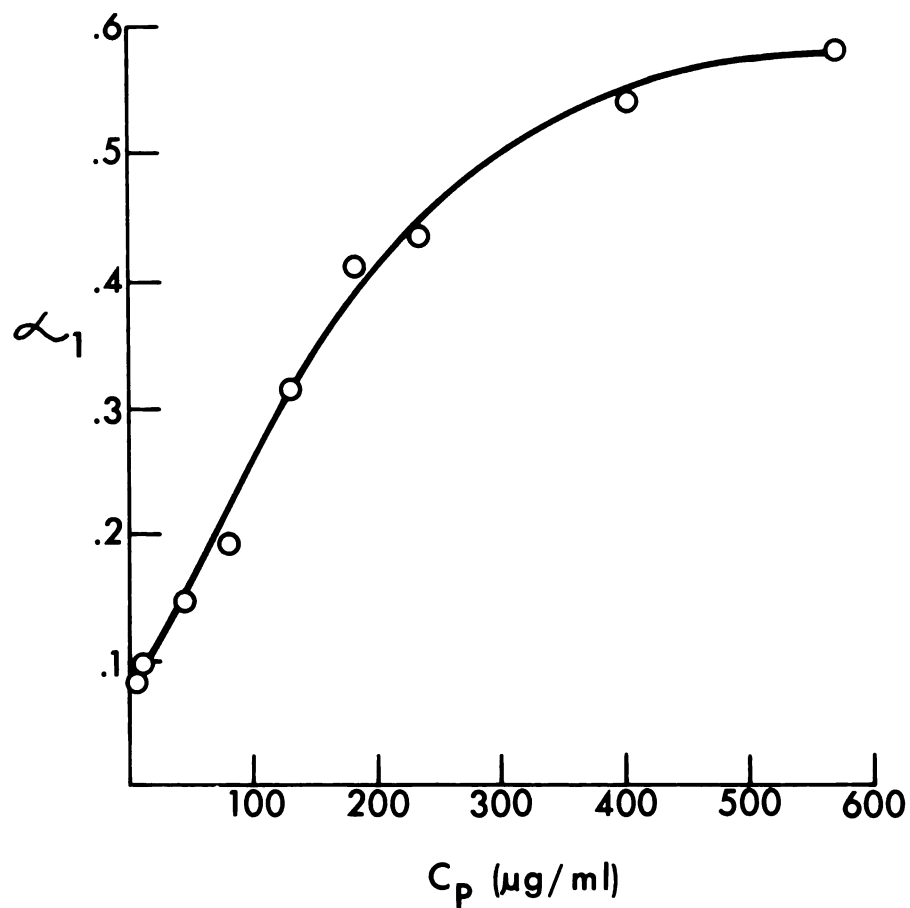


Figure 3-4. Unbound fraction of total plasma concentration,  $\alpha_1$ , as a function of the total plasma concentration,  $C_p$ .

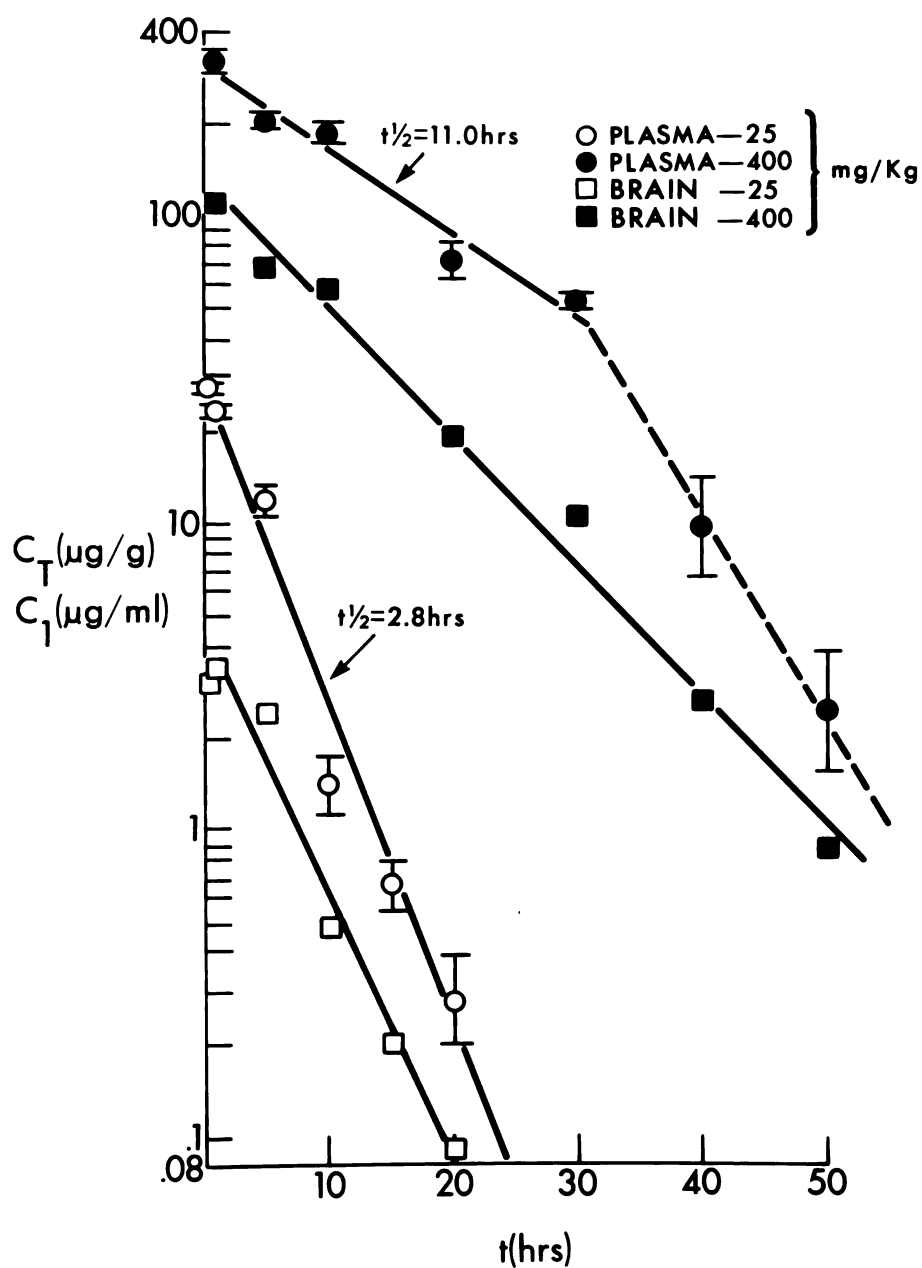


Figure 3-5. Semi-logarithmic plots of salicylic acid concentrations in rat brain and plasma versus time after intraperitoneal administration of 25 and 400 mg/kg.  $C_1$  is the unbound concentration of salicylic acid in the plasma;  $C_T$  is the concentration of salicylic acid in the brain corrected for residual blood.

## CHAPTER IV

### SUMMARY AND CONCLUSIONS

The objective of the work which was carried out was multifold. The primary goal was the study of the acid transport system(s) in the brain and its possible involvement as a functional component of the blood-brain barrier. It was desired, however, to accomplish this study utilizing techniques which did not have the drawbacks of most research involving the brain, that is, disruption of the blood-brain barrier. Published research dealing with transport systems in the brain invariably utilize one or more of the following procedures:

- 1) Ventricular-cisternal perfusions consist of introducing a solution of a drug into the ventricles. Samples are taken from the cisterna magna or from the general circulation of the animal being used. The much quoted work by Pappenheimer (17) in which it was shown that Diodrast and phenolsulfonylphthalein are actively transported out of the cerebrospinal fluid, utilized this technique. The facility by which metabolic or competitive inhibitors can be added to the perfusion medium coupled with the ability to study transport against concentration gradients makes this technique very useful when attempting to demonstrate that an active transport exists. While useful, this procedure has the disadvantage of requiring

surgery to implant cannulas into the ventricles and the cisterna magna. Thus, the animal must be sedated before the experiment can be carried out. If the animal is allowed to recover from sedation, it must then be restrained to maintain the cannulas in place, and the animal is not in a normal state. Besides the inherent problems that can arise with surgery, there is also the possibility of altering the normalcy of the blood-brain barrier by introduction of the cannulas. The method of introducing the drug into the brain bypasses the normal routes of drug entry into the brain, and this also must be considered a major disadvantage. Furthermore, experiments utilizing this technique are really studying transport from the cerebrospinal fluid to blood and not from the brain parenchyma to blood and vice versa.

2) Brain slice incubation involves slicing the brain into thin slices which can then be incubated in drug solutions over a period of time to allow the brain parenchyma to come to an equilibrium with the drug solution. If the ratio of brain concentration (corrected for binding) to drug solution is greater than one, an active uptake of the compound being tested can be postulated. If the ratio is less than one, the possibility exists that the brain inhibits the absorption of the drug by some mechanism such as a transport system. Metabolic inhibitors and competitive transport inhibitors can be added to the incubation medium to prove the presence or absence of transport systems. This technique has been extensively used, especially by Lajtha in his studies involving the uptake of

amino acids by the brain (37, 38). The artificiality of an in vitro study with brain slices as compared to the complex system of a living brain should be readily apparent. Physical or anatomical barriers to drug diffusion between the blood and the brain will not be detectable with this technique. Also, carrier-mediated systems may lose their ability to transport drugs in vitro, especially if an essential cofactor is missing. If a mechanism for transport should exist between the cerebrospinal fluid and blood, this procedure might completely obliterate it.

3) Incubations of choroid plexuses have been used to prove the involvement of the choroid plexus in the transport of compounds from the cerebrospinal fluid to the blood and in the uptake of compounds from the blood to the cerebrospinal fluid. The arguments presented against brain slice incubations are also applicable in this case. In addition, another problem arises. While a choroid plexus incubation might demonstrate a transport mechanism from the cerebrospinal fluid to blood or in the direction of blood to the cerebrospinal fluid, it could not possibly show anything concerning mechanisms which exist between the brain parenchyma and the blood. This technique, along with brain slice incubations, has the added disadvantage of limiting the studies which may be carried out with endogenous compounds, since the metabolic activity of an isolated system is at best questionable.

The procedures utilized in the present study do not suffer from any of the drawbacks listed above. In the case



of the 5HIAA accumulation studies, the only drug administered was probenecid, and it was administered intraperitoneally, not directly into the central nervous system. By studying the accumulation of brain 5HIAA there was no need to introduce any compounds into the central nervous system since 5HIAA is a normal metabolic product of the putative neurotransmitter serotonin. 5HIAA thus served as an endogenous tool to study the acid transport system in the brain. The rats used in this study were handled only at the time of injection and sacrifice; thus, they suffered no trauma during the course of an experiment comparable to ventricular-cisternal cannulation. Furthermore, after administration of the probenecid dose the rats behaved perfectly normal when returned to their cages, and had free access to water and food, a situation hardly comparable to sedation or restriction.

In the studies involving salicylic acid entry into the brain, the rats received the drug through an intraperitoneal injection and were sacrificed by decapitation, essentially the same experimental procedure used in the 5HIAA studies. In these studies, as in the ones involving 5HIAA transport, the rats had free access to water and food. They also demonstrated their normal grooming and social behavior even after receiving the 400 mg/kg dose; a particularly good sign in view of the fact that overdosing by salicylates manifests itself in the form of convulsions.

Another goal or objective was to demonstrate that endogenous and exogenous acids are transported out of the brain by similar transport or carrier-mediated systems. From a teleological viewpoint, it would seem reasonable that only one system would exist for the disposal of unwanted acids whether they are acids produced in the brain or those which enter the brain from the general circulation. The acid transport system probably developed along with the evolution of the central nervous system as a mechanism to protect the brain from endogenously formed acids, that is, those produced through metabolism. For biochemical economy this system could also function to rid the brain of unwanted exogenous acids or those compounds which enter the brain from the blood. It is thus reasonable that the system which functions to rid the brain of acidic metabolites should be identical to that which prevents the accumulation of foreign organic acids. While the conclusive proof of this latter objective might be very difficult, some insight into the plausibility of this theory could be obtained if models based on a similar mechanism could be developed to describe the transport of endogenous and exogenous acids.

Utilizing this approach, models based on the involvement of a carrier mediated transport system have been developed for both the experiments with 5HIAA and salicylic acid. Figure 2-1 has been previously cited to demonstrate how the levels of 5HIAA fluctuate after the administration of a 100 mg/kg dose of probenecid. Since probenecid is a known

inhibitor of acid transport systems, it is highly likely that the accumulation of 5HIAA as depicted in Figures 2-9 and 2-10 is a result of inhibition of the transport system which normally excretes 5HIAA out of the brain. In Figure 2-11, the accumulation of 5HIAA was much greater since a large dose, 300 mg/kg, was used. One explanation could simply be that the higher levels of probenecid produced a higher degree of inhibition for a longer period of time. Another rationale could be based on the longer half life of elimination that was observed for probenecid after the 300 mg/kg dose. The longer half life for the inhibitor would allow a longer duration of inhibition and a higher 5HIAA accumulation. To test this possibility, the model as described by Equation 9 was changed into an analog computer diagram as has been described in Chapter II. However, instead of generating computer curves to fit the 5HIAA brain data as was done with Figures 2-9, 2-10, and 2-11, different values for  $k_I$ , the rate constant of elimination for probenecid, were introduced into the computer. The 5HIAA brain levels generated by the computer may be seen in Figure 4-1. This figure readily demonstrates the different extent of 5HIAA accumulation when different rate constants of elimination are used. It should be noted that the degree of accumulation of 5HIAA was influenced solely by increasing the half life of the inhibitor without changing  $K_I$  or the level of the inhibitor. It is important to reemphasize that this figure is theoretical and not intended to fit any data; however, the computer curves shown on Figures

2-9, 2-10, and 2-11 are superimposed over real data. The model that was used to generate these curves assumed the existence of a transport system capable of being competitively inhibited. Since the model fit the data obtained in vivo reasonably well, it can be said that this model approximates the in vivo situation. The concept of a carrier mediated transport system must then be sound.

The susceptibility to inhibition is a trait of a carrier mediated transport system as is saturability. As discussed above, the 5HIAA transport system can be readily inhibited by probenecid. The salicylic acid experiments, on the other hand, demonstrated the saturability of the acid transport system. The derivation of the distribution ratio,  $R$ , is based on the concept that the ratio between drug in the plasma and brain should be unity if the processes involved in the entry and exit of salicylic acid are all passive. Increasing the amount of the exogenous compound, salicylic acid, in the blood should have no effect on the ratio of drug in brain to drug in plasma if no saturable processes are involved. If the ratio does change with increasing or decreasing doses of salicylic acid, processes other than passive must exist. As discussed in Chapter III, the fact that the  $R$ 's are seen to increase points to the saturation of a transport system in the direction of brain to blood. Utilizing the data from Sturman, et al. (33) and McArthur, et al. (34), it was demonstrated that the distribution ratios increased with increasing dose and that they approached unity. The lack of

equality of the distribution ratios when different doses were used suggests the existence of a saturable transport system. If such a transport system became saturated, it would then be possible for the levels in the brain to reach a dynamic equilibrium with the salicylic acid in the plasma. A distribution ratio of one would be expected if the transport system became completely saturated. The  $R$ 's listed in Table XI approach unity, thus lending substance to the theory that salicylic acid in the brain does not achieve equilibrium with salicylic acid in the plasma because of an acid transport system which excretes salicylic acid out of the brain.

It should be emphasized that the unbound concentration of salicylic acid in plasma should be compared to the brain concentrations rather than the total concentration in plasma. The reason for this is that only the unbound drug is capable of diffusing into the brain from the general circulation; as a result, only the unbound salicylic acid is free to equilibrate with the salicylic acid in the brain. The ideal experimental design would be to compare the levels of salicylic acid in the brain with the unbound plasma concentration when the plasma levels are kept at a steady state. In lieu of such an experiment, the calculations of the  $R_{\text{COR}}$  and  $R_{\text{COR}}^{\text{max}}$  values were carried out. The rationale for the use of  $R_{\text{COR}}$  and  $R_{\text{COR}}^{\text{max}}$  calculations has been presented in Chapter III, Section 2, Theoretical. If a saturable transport system did not exist, all the  $R_{\text{COR}}$  and  $R_{\text{COR}}^{\text{max}}$  values reported in Tables X and XI should be equal. This of course is not the case. The

$R_{\text{COR}}$  and  $R_{\text{COR}}^{\text{max}}$  values are seen to increase with dose, thus suggesting the presence of a transport system in the direction of brain to blood. Furthermore, since the  $R_{\text{COR}}^{\text{max}}$  values in Table XI approach unity, the saturability of the transport system is seen to be plausible.

At any one time point, the concentrations of unbound salicylic acid per milliliter of plasma were always higher than the corresponding concentrations per gram of brain tissue. Yet the acid transport system in the brain apparently was capable of continuing to remove salicylic acid from the brain; the transport system was able to operate against a concentration gradient. If the transport mechanism eliminates salicylic acid from the brain directly into the blood, it would suggest that the system is an active transport, for it is moving the salicylic acid from an area of lower concentration to one of higher concentration.

Metabolism of salicylic acid in the brain was ruled out as a mechanism for the elimination of salicylic acid from the brain in Chapter III. Elimination of salicylic acid by bulk flow of the cerebrospinal fluid was also considered unlikely, since the turnover of the cerebrospinal fluid is a slow process in comparison to the turnover of salicylic acid. The rate of turnover for the cerebrospinal fluid is about 10 percent per hour (39, 40) while salicylic acid is 50 percent in 2-3 hours after a 25 mg/kg dose in rats. Also, if salicylic acid were eliminated through cerebrospinal fluid bulk flow, the distribution ratios would not be

dose-dependent since the fluid bulk flow is not a saturable process.

The very rapid turnover of 5HIAA, 85 percent per hour, has been previously reported (20). This also provides support to the concept that the cerebrospinal fluid could not possibly be involved to a major extent in the elimination of 5HIAA from the brain. For the turnover time of 5HIAA to be so short, it would require the transport system to exist directly between the brain parenchyma and the blood. If diffusion of 5HIAA were involved in its elimination, it could not occur over great distances, since diffusion is a slow process relative to the turnover rate of 5HIAA. Cerebrospinal fluid involvement must therefore be minor. The 5HIAA transport studies substantiate the salicylic acid studies, which suggest that the transport must be an active process which operates in moving acidic compounds from the brain tissue into the blood.

An added benefit of the 5HIAA experiments was the quantitation of the inhibition of the transport system by probenecid. This resulted from the computer fits of the 5HIAA brain concentration-time curves. Different curves were generated for each set of data points by varying the constant of inhibition,  $K_I$ ; the curve which best fit the data was that which had been generated utilizing the proper  $K_I$ . The constant of inhibition,  $K_I$ , for the purposes of this discussion was defined as the plasma concentration of probenecid which produced 50 percent inhibition of the transport of 5HIAA.

The  $K_I$  values calculated from the computer fits have

been listed in Table VI. The values obtained were quite similar, although the probenecid elimination half lives varied with dose. The dose-dependency of probenecid is an interesting concept in itself which has been previously reported (28). The results of this study seem to verify the drug's dose-dependent kinetics since the half life of probenecid increased by a factor of four when the dose was increased from 100 to 300 mg/kg. It would appear that further study of this property of probenecid would be of great value.

The  $K_I$  value was also determined by a calculation technique illustrated by Figure 2-12. The values for  $K_I$  which resulted from the two different techniques correlated well. The average of the  $K_I$ 's from the computer fits was 55  $\mu\text{g}/\text{ml}$ ;  $K_I$  from the percent inhibition calculations worked out to be 80  $\mu\text{g}/\text{ml}$ .

With regard to the experiments involving the administration of salicylic acid, it was initially desired only to verify the existence of a transport system in the brain for exogenous acids. As the study developed, the quantitations of the transport of exogenous acids evolved into a technique which should detect the presence of any saturable process including transport. This technique, as discussed in Chapter III, should be applicable not only for detecting transport in the brain, but also to detect any saturable process which would result in the nonlinear disposition of a drug in any tissue.

Regardless of the procedure utilized in the study of the brain's acid transport system, the results provide substantial evidence for a system which is active, carrier mediated, and located such that it removes organic acids from the brain directly to the blood.



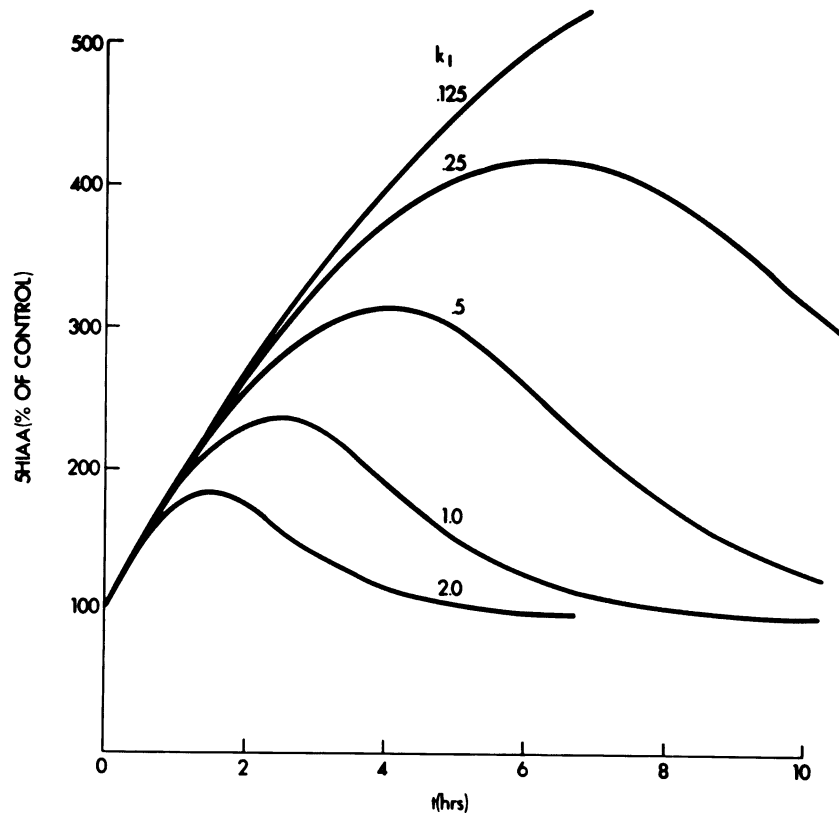


Figure 4-1. Analog computer curves representing 5HIAA brain levels as a function of time. These curves were generated by varying only the value of  $k_1$  in the model.

## APPENDIX A

### MODEL AND ANALOG COMPUTER DIAGRAM USED IN THE DETERMINATION OF $K_I$

Equation 9 from Chapter II is the rate equation which served as a model for 5HIAA elimination from the brain. This equation assumes the existence of a 5HIAA transport system which is susceptible to inhibition. The model is given below.

$$\left(\frac{dA}{dt}\right)_I = R_{\text{syn}} - \frac{kC_A}{1 + \frac{C_{I_0}e^{-k_I t}}{K_I}}$$

where  $\left(\frac{dA}{dt}\right)_I$  is the change in the amount of 5HIAA with time in the presence of the inhibitor probenecid. The rate of synthesis of 5HIAA is represented by  $R_{\text{syn}}$ ;  $k$  is the rate constant for 5HIAA elimination, and  $C_A$  is the concentration of 5HIAA in the brain. The constant of inhibition for probenecid is  $K_I$ ;  $C_{I_0}$  is the plasma concentration of probenecid obtained by extrapolation of the plasma concentration curve to zero time, and  $k_I$  is the rate constant for probenecid elimination from the rat. All the values in this equation, with the exception of  $K_I$ , can be obtained either from literature information or from the experimental data obtained from this study. The 5HIAA synthesis rate was obtained from the product of the rate constant for 5HIAA elimination and the steady state level of 5HIAA. The value used for  $k$  was  $0.92 \text{ hr}^{-1}$ .

The final scaled equation used in the analog computer follows:

$$\frac{\dot{A}}{5} = \frac{R_{\text{syn}}}{(10)5} - \frac{k \frac{C_A}{5}}{20 \left( \frac{1}{20} + \frac{C_I \cdot e^{-K_I t}}{20K_I} \right)}$$

Figure A-1 is the computer diagram used to generate curves representing the change in the levels of brain 5HIAA with time. By varying the value for  $K_I$ , different curves were produced until the best fit of the in vivo data was obtained. The curve of best fit corresponds to the correct  $K_I$ .

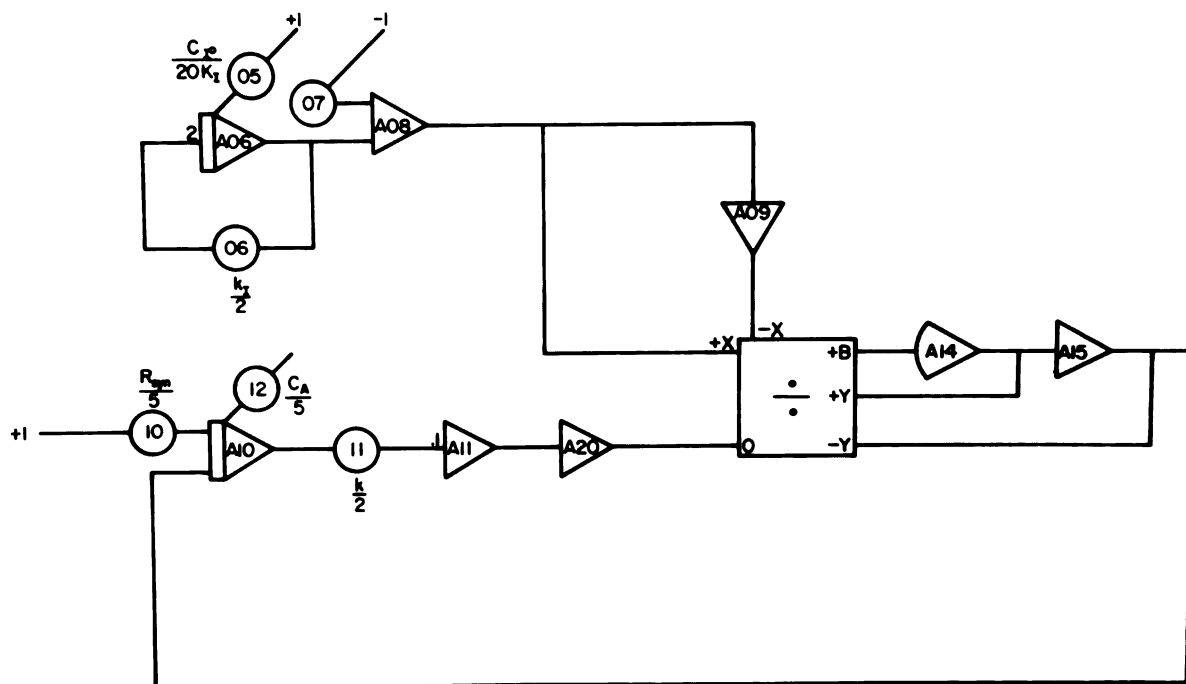


Figure A-1. Analog computer diagram used to represent the change in 5HIAA brain levels after a dose of probenecid. The triangles represent amplifiers; the circles represent potentiometers.

## APPENDIX B

### CORRECTION FOR RESIDUAL BLOOD IN BRAIN

Extraction of salicylic acid from brain homogenates had an inherent error due to residual blood in the brain after decapitation of the rats. Literature reports cite the volume of residual blood as 11  $\mu$ l per gram of brain tissue for rats sacrificed by decapitation (31). To correct the brain concentrations for the amount of salicylic acid contributed by the residual blood it was necessary to multiply 11  $\mu$ l by the concentration of salicylic acid in blood and subtract the amount obtained from the assayed value for brain salicylic acid.

In the studies involving the transport of salicylic acid, plasma concentrations were determined rather than blood concentrations. It therefore became necessary to carry out a study to determine the level of salicylic acid in the blood at a certain plasma concentration. The experimental procedure utilized was the following. Samples were prepared consisting of 2 ml of fresh whole blood from rats to which was added known amounts of salicylic acid dissolved in 0.1 ml of Krebs-Ringer bicarbonate buffer. The samples were gently shaken while they were incubated for one hour in a water bath at 37°C. After incubation they were centrifuged at 1300 x g for 5 minutes to separate the plasma from the blood cells. One ml of plasma was transferred from each sample into

centrifuge tubes containing 1 ml of a 5 percent solution of potassium bisulfate. This resulted in acidification of the plasma. A volume of 5 ml of ether was added to the samples, and they were then shaken for 15 minutes on a Lab-Tek<sup>®</sup> mixer. After shaking the samples were centrifuged for 5 minutes. An aliquot of 1 ml from the ether layer was then transferred into another centrifuge tube containing 5 ml of a 0.5 M phosphate buffer with a pH of 7.0. The samples were shaken again for 15 minutes and centrifuged. Using a Pasteur pipette, an aliquot from the phosphate buffer layer was removed from each sample to read the fluorescence. The fluorescence assay for salicylic acid has been previously described in Chapter III under Section 3: Experimental. Table XII summarizes the results of this study. The blood concentration values listed were obtained by dividing the amount of salicylic acid added by 2.1 ml, the final volume of the sample. The plasma concentration values listed in Table XII are the results of the salicylic acid assay described above.

The hematocrit of rat blood samples was determined by centrifugation at 1300 x g for 30 minutes. The average hematocrit obtained was 0.40. Thus the plasma represents about 60 percent of the whole blood. Since the plasma concentrations listed in Table XII are usually higher than the blood concentrations, it can be said that the distribution of salicylic acid in the blood is not uniform. The drug appears to concentrate in the plasma; this is to be

TABLE XII  
BLOOD AND PLASMA CONCENTRATIONS UPON ADDING  
SALICYLIC ACID TO RAT BLOOD

Blood Concentration ( $\mu\text{g/ml}$ )	Plasma Concentration ( $\mu\text{g/ml}$ )
7.62	13.09
19.05	31.21
38.10	57.21
95.24	125.69
172.62	216.89
476.19	489.13
952.38	928.67

expected since salicylic acid undergoes plasma protein binding.

The amount of salicylic acid in the blood and its distribution can be described by the following equation:

$$C_B V_{B\ell} = C_P V_{B\ell} (1-H) + [\text{RBC}] V_{B\ell} H \quad (1)$$

where  $C_B$  is the concentration of salicylic acid in the blood, and  $V_{B\ell}$  is the volume of the blood; the product of these two values equals the total amount of salicylic acid in the blood. The concentration of the drug in the plasma is  $C_P$ ;  $H$  is the hematocrit value, and  $[\text{RBC}]$  is the concentration of salicylic

acid in the red blood cells or the cellular portion of the blood. Simple manipulation of Equation 1 leads to a relationship which can be utilized to convert the plasma concentration values obtained in the salicylic acid transport experiments to blood concentrations.

Dividing Equation 1 by  $C_P V_B$  yields the following:

$$\frac{C_B}{C_P} = (1-H) + \frac{[RBC]H}{C_P} \quad (2)$$

The fraction of a drug's concentration unbound in the plasma,  $\alpha_1$ , was defined in Chapter III as the unbound concentration,  $C_1$ , divided by the total concentration in the plasma,  $C_P$ .

Therefore,

$$C_P = \frac{C_1}{\alpha_1} \quad (3)$$

Substituting Equation 3 into Equation 2 produces the following equation:

$$\frac{C_B}{C_P} = (1-H) + \frac{H[RBC] \alpha_1}{C_1} \quad (4)$$

If the ratio of  $[RBC]/C_1$  is a constant then a linear relationship is expressed by Equation 4; that is, plotting  $C_B/C_P$  versus  $\alpha_1$  should yield a linear plot whose slope is  $H[RBC]/C_1$ , and the y-intercept is  $(1-H)$ .

The data in Table XII was utilized to test the validity of Equation 4. Dividing the blood concentration values by the corresponding plasma concentrations produced values for  $C_B/C_P$ . For each plasma concentration listed in Table XII a value for  $\alpha_1$  was obtained from Figure 3-4. The results of



plotting  $C_B/C_P$  versus  $\alpha_1$  may be seen in Figure B-1. The correlation coefficient obtained by linear regression was found to be 0.992. The hematocrit value calculated from the y-intercept of Figure B-1 was 0.48, which compares favorably with the experimental value of 0.40.

Using Figure B-1 it was then possible to convert the plasma concentrations obtained in the salicylic acid transport studies to blood concentrations. For each plasma concentration an  $\alpha_1$  was determined from Figure 3-4. By referring to Figure B-1, a value of  $C_B/C_P$  was calculated for each  $\alpha_1$  value. The ratio  $C_B/C_P$  was then multiplied by the assayed plasma concentration from the transport studies to obtain the blood concentration. These blood concentrations were then used to correct for the salicylic acid in the brain contributed by the residual blood.

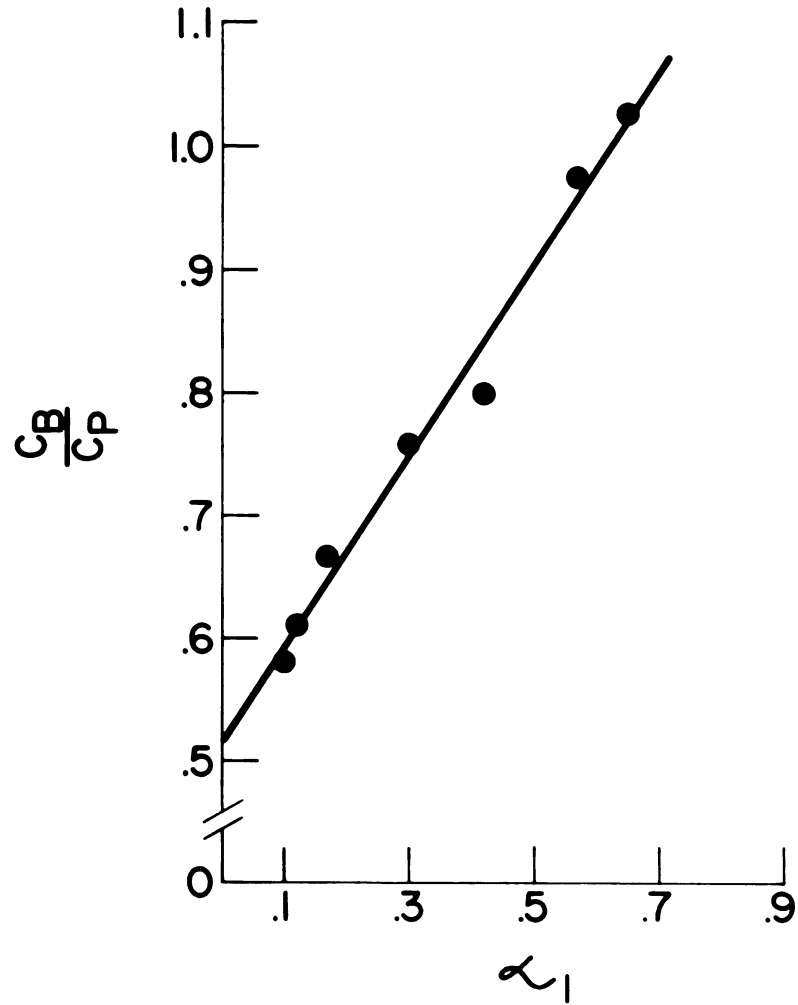


Figure B-1. Ratio of salicylic acid blood concentration ( $C_B$ ) to plasma concentration ( $C_P$ ) as a function of the fraction of drug unbound in the plasma ( $\alpha_1$ ).

## BIBLIOGRAPHY

1. Ehrlich, P. "Ueber provocirte Fluorescenzerscheinungen am Auge." Dtsch. med. Wschr, 8: 21,35,54 (1882).
2. Lewandowsky, M. "Zur Lehre der Cerebrospinalflüssigkeit." Z. Klin. Med., 40: 480 (1900).
3. Goldmann, E.E. "Die äussere und innere Sekretion des gesunden und Kranken Organismus im Lichte der Vitalen Farbung." Beitr. Klin. Chirurg., 64: 192 (1909).
4. Wallace, G.B. and Brodie, B.B. "The distribution of iodide, thiocymate, bromide and choride in the central nervous system and spinal fluid." J. Pharmacol., 65: 220 (1939).
5. Mayer, S., Maickel, R.P. and Brodie, B.B. "Kinetics of penetration of drugs and other foreign compounds into cerebrospinal fluid and brain." J. Pharmacol., 127: 205 (1959).
6. Brodie, B.B., Kurz, H. and Schanker, L.S. "The importance of dissociation constant and lipid-solubility in influencing the passage of drugs into the cerebrospinal fluid." J. Pharmacol., 130: 20 (1960).
7. Horstmann, E. and Mevesi, H. "Die Feinstruktur des molekularen Rindengraves und ihre physiologische Bedeutung." Z. Zellforsch, 49: 569 (1959).
8. Rall, D.P., Oppelt, W.W. and Patlak, C.S. "Extracellular space of brain as determined by diffusion of insulin from the ventricular system." Life Sci., 2: 43 (1962).
9. Wolff, J. "Beiträge zur Ultrastruktur der Kapillaren in der normalen Grosshirnrinde." Z. Zellforsch, 60: 409 (1963).
10. Cserr, H.F., Fenstermacher, J.D. and Rall, D.P. "Permeabilities of the choroid plexus and blood-brain barrier to urea." Proc. Int. Colloquium on Urea and the Kidney, Sarasota, Florida. Excerpta Medica, Amsterdam, 127 (1970).
11. Kleeman, C.R., Davson, H. and Levin, E. "Urea transport in the central nervous system." Amer. J. Physiol., 203: 739 (1962).
12. Steinwall, O. "Transport inhibition phenomena in unilateral chemical injury of blood-brain barrier," in Brain Barrier Systems, A. Lajtha and D. H. Ford, Eds. Elsevier Publishing Company, New York, 1968, pp. 357-365.

13. Steinwall, O. "Transport mechanisms in certain blood-brain barrier phenomena - a hypothesis." Acta. psychiat. scand., 36: Suppl. 150,314 (1961).
14. Dumoff-Stanley, E., Dowling, H.F. and Street, L.K. "The absorption into and distribution of penicillin in the cerebrospinal fluid." J. clin. Invest., 25: 87 (1946).
15. Belsey, M.A. and Tardo, C. "Cerebrospinal fluid levels of ampicillin and penicillin during pneumococcal meningitis: Experimental studies in dogs." Ann. N.Y. Acad. Sci., 145:2, 482 (1967).
16. Fishman, R.A. "Blood-brain and CSF barriers to penicillin and related organic acids." Arch. Neurol., 15: 113 (1966).
17. Pappenheimer, J.R., Heisey, S.R. and Jordan, E.F. "Active transport of diodrast and phenolsulfonphthalein from cerebrospinal fluid to blood." Am. J. Physiol., 200: 1,1 (1961).
18. Tozer, T.N., Neff, N.H. and Brodie, B.B. "Application of steady-state kinetics to the synthesis rate and turnover time of serotonin in the brain of normal and reserpine-treated rats." J. Pharmacol. Exp. Therap., 153: 177 (1966).
19. Neff, N.H., Tozer, T.N. and Brodie, B.B. "Application of steady-state kinetics to studies of the transfer of 5-Hydroxyindoleacetic acid from brain to plasma." J. Pharmacol. Exp. Therap., 158: 214 (1967).
20. Neff, N.H. and Tozer, T.N. "In vivo measurement of brain serotonin turnover," in Advances in Pharmacology, Vol. 6A, S. Garattini and P. A. Shore, Eds., Academic Press, New York, 1968, pp. 97-109.
21. Andersson, H. and Roos, B.E. "5-Hydroxyindoleacetic acid in cerebrospinal fluid after administration of 5-Hydroxytryptophan I." Acta. pharmacol. et toxicol., 26: 293 (1968).
22. Bowers, M.B. Jr. and Gerbode, F. "CSF 5-HIAA: Effects of probenecid and parachlorophenylalanine." Life Sci., 7: 773 (1969).
23. Guldberg, H.C., Ashcroft, G.W. and Crawford, T.B.B. "Concentrations of 5-Hydroxyindolylacetic acid and homovanillic acid in the cerebrospinal fluid of the dog before and during treatment with probenecid." Life Sci., 5: 1571 (1966).

24. Anderson, H. and Roos, B.E. "The effect of probenecid on the elimination from CSF of intraventricularly injected 5-hydroxyindoleacetic acid in normal and hydrocephalic dogs." J. Pharm. Pharmacol., 20: 879 (1968).
25. Tozer, T.N., Personal communication based on unpublished data from 1966.
26. Roos, B.E. "On the occurrence and distribution of 5-hydroxyindoleacetic acid in brain." Life Sci., 1: 25-27 (1962).
27. Udenfriend, S., Weissbach, H. and Brodie, B.B. "Assay of serotonin and related metabolites, enzymes and drugs," in Methods of Biochemical Analysis, ed. by D. Glick, Interscience Publishers, New York, 1958, pp. 95-130.
28. Dayton, P.G., Yu, T.F., Chen, W., Berger, L., West, L.A. and Gutman, A.B. "The physiological disposition of probenecid including renal clearance, in man, studied by an improved method for its estimation in biological material." J. Pharmacol. Exp. Therap., 140: 3, 278 (1963).
29. Tozer, T.N. and Kimble, D., Personal communication based on unpublished data from 1967.
30. Rowland, M. and Riegelman, S. "Determination of acetylsalicylic acid and salicylic acid in plasma." J. Pharm. Sci., 56: 6, 717 (1967).
31. Muelheims, G., Dellenback, R. and Rawson, R. "Red blood cell volume and distribution after bleed-out in the rat as determined by Cr<sup>51</sup>-labeled red blood cells." Amer. J. of Physiol., 196: 169 (1959).
32. Levy, G., Tsuchiya, T. and Amsel, L.P. "Limited capacity for salicyl glucuronide formation and its effect on the kinetics of salicylate elimination in man." Clin. Pharmacol. Ther., 13:2, 258 (1972).
33. Sturman, J.A., Dawkins, P.D., McArthur, N. and Smith, M.J.H. "The distribution of salicylate in mouse tissues after intraperitoneal injection." J. Pharm. Pharmacol., 20: 58 (1968).
34. McArthur, J.N., Dawkins, P.D. and Smith, M.J.H. "The relation between circulating and tissue concentrations of salicylate in the mouse in vivo." J. Pharm. Pharmacol., 22: 801 (1970).

35. Wolff, J. and Austen, F.K. "Salicylates and thyroid function. II. The effect on the thyroid-pituitary interrelation." J. Clin. Invest., 37: 1144 (1958).
36. Smith, M.J.H. and Smith, P.K. The Salicylates. Interscience Publishers, New York, 1966, pp. 58-61.
37. Lajtha, A. and Toth, J. "The brain barrier system. V. Stereospecificity of amino acid uptake, exchange and efflux." J. Neurochem., 10: 909 (1963).
38. Battistin, L., Grynbaum, A. and Lajtha, A. "Energy dependence of amino acid uptake in brain slices." Brain Research, 16: 187 (1969).
39. Davson, H. "The secretion of the cerebrospinal fluid," in Physiology of the Cerebrospinal Fluid, Little Brown and Company, Boston, 1967.
40. Goldstein, A., Aronow, L. and Kalman, S.M. "The absorption, distribution, and elimination of drugs," in Principles of Drug Action, Harper and Row, Publishers, Inc., New York, 1969.

